

Analysis of the Naphthalene Vapour Absorption Bands at 3200 angstrom I. Naphthalene h-8

D. P. Craig, J. M. Hollas, M. F. Redies and S. C. Wait

Phil. Trans. R. Soc. Lond. A 1961 **253**, 543-568

doi: 10.1098/rsta.1961.0009

Email alerting service

Receive free email alerts when new articles cite this article - sign up in the box at the top right-hand corner of the article or click [here](#)

ANALYSIS OF THE NAPHTHALENE VAPOUR ABSORPTION
BANDS AT 3200 ÅI. NAPHTHALENE *h*-8BY D. P. CRAIG, J. M. HOLLAS,* M. F. REDIES‡
AND S. C. WAIT, JR†*Sir William Ramsay and Ralph Forster Laboratories, University College, London
and**‡Department of Physical Chemistry, University of Sydney, Australia**(Communicated by Sir Christopher Ingold, F.R.S.—Received 13 September 1960—
Read 9 March 1961)*

[Plates 9 and 10]

CONTENTS

	PAGE		PAGE
EXPERIMENTAL	545	DISCUSSION (<i>cont.</i>)	
RESULTS	546	Bands originating at the false origin 0 + 911 cm ⁻¹	556
DISCUSSION	548	Occurrence of sequences: ground-state vibrations	556
The band contours	548	Other principal band heads	558
The hot bands	551	Comparison with solid-state spectra	558
Vibrational structure: progressions	554	REFERENCES	561
Bands originating at the electronic origin	555	APPENDIX	562
Bands originating at the false origin 0 + 438 cm ⁻¹	555		

The absorption bands of naphthalene vapour near 3200 Å have been measured at medium and high resolution and analyzed for the first time. The bands have strong heads weakly degraded to the red. The direction of polarization of the 0-0 pure electronic transition has been identified from the band contour of the corresponding band, which shows a single intense maximum. Calculations of rotational energy levels confirm that this is a quasi-parallel *A*-type band of the asymmetric rotor, with polarization along the longer in-plane molecular axis. Accompanying the electronically allowed band is a set of stronger vibrationally induced bands, which show doubled intensity maxima. From approximate calculations of contours it is confirmed that these are quasi-perpendicular *B*-type bands, polarized along the shorter in-plane axis. The electronic assignment $B_{2u} \leftarrow A_g$, long-axis polarized, agrees with McClure's assignment from the spectrum of naphthalene embedded in durene crystals. The use of rotational band contours for assigning transitions is novel in larger molecules and seems likely to be applicable rather widely.

A hitherto unrecorded ground-state frequency 506 cm⁻¹ of species b_{3g} has been identified, and a number of other ground and excited-state frequencies confirmed and assigned, or recorded for the first time.

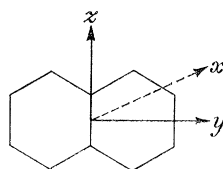
* Present address: Division of Pure Physics, National Research Council, Ottawa, Canada.

† Present address: National Bureau of Standards, Washington 25, D.C., U.S.A.

The naphthalene bands near 3200 Å record a weak transition, of oscillator strength $f \approx 0.002$. They were photographed in absorption in a careful study by Henri & de Laszlo in 1924, but no comprehensive analysis of the measured bands has ever been published. Spomer & Nordheim (1950) and Knipe, Spomer & Cooper (1953), remeasured the spectrum in the vicinity of the origin band and made some measurements of the corresponding system of naphthalene *d*-8. Further measurements were reported by Prikhotjko (1949). The vapour fluorescence was measured by Schnepf & McClure (1952) and a number of the bands assigned.

Solid-state spectra of this naphthalene transition have been thoroughly measured and analyzed. The earlier references are given by Prikhotjko (1944), who measured the system in absorption in the pure crystal. McClure's work (1954) on the absorption of naphthalene embedded in durene was of outstanding importance. McClure showed that, on certain assumptions about the orientation of the naphthalene molecules in the host crystal, the pure electronic band is polarized parallel to the longer in-plane axis, but the stronger bands of the system are all short-axis polarized and must correspond to vibration-induced transitions. Similar methods were applied to mixed crystal fluorescence, and to mixed crystals containing naphthalene *d*-8 (McClure 1956).

As to the outcome of these studies, it can be said that the assignment of this transition of naphthalene to the long-axis polarized species $B_{2u} \leftarrow A_g$ is firmly based. However, the analyses of the observed solid-state spectra that have been proposed in accordance with the assignment are all in some respects objectionable. We have therefore sought to clarify the issues by making a careful study of the vapour bands, and can now propose a fairly complete analysis which confirms the assignment, and disposes of the difficulties of previous work. A number of upper-state frequencies have been identified, a new ground-state frequency at 506 cm^{-1} located and assigned, and another at 936 cm^{-1} confirmed and reassigned, in addition to those so far recorded in Raman and infra-red spectra.



The symmetry notation follows throughout the recommendations of the Joint Commission for Spectroscopy (1955). The axes adopted are shown in the diagram, and the D_{2h} group representations listed in table 1.

TABLE 1. SYMMETRY SPECIES FOR GROUP D_{2h}

	E	$\sigma(xy)$	$\sigma(xz)$	$\sigma(yz)$	i	$C_2(z)$	$C_2(y)$	$C_2(x)$
A_g	+1	+1	+1	+1	+1	+1	+1	+1
A_u	+1	-1	-1	-1	-1	+1	+1	+1
B_{1g}	+1	+1	-1	-1	+1	+1	-1	-1
B_{1u}	+1	-1	+1	+1	-1	+1	-1	-1
B_{2g}	+1	-1	+1	-1	+1	-1	+1	-1
B_{2u}	+1	+1	-1	+1	-1	-1	+1	-1
B_{3g}	+1	-1	-1	+1	+1	-1	-1	+1
B_{3u}	+1	+1	+1	-1	-1	-1	-1	+1

EXPERIMENTAL

The naphthalene used was cryoscopic grade material recrystallized from alcohol after treatment with Raney nickel to remove sulphur-containing impurities.

Measurements were made with a Hilger large quartz spectrograph *E492*, and with the Ebert 20 ft. grating spectrograph described by King (1958). Two absorption cells were used for the measurements at lower dispersion (in the quartz spectrograph). The first was a White multiple reflexion cell (White 1942) with 3 ft. between front surface aluminized mirrors. This was satisfactory up to 16 passes at 3000 Å and was used from room temperature to 40 °C. For higher temperature studies of the hot bands a single-pass 12 ft. cell was made from 2 in. diam. Pyrex tubing with silica windows attached by brass adaptors and silicone rubber O-rings. A bulb reservoir for naphthalene could be held at constant temperature by immersion in the vapour of a suitable refluxing solvent. The cell itself was wound helically with Nichrome wire over spaced strands of asbestos cord and covered with asbestos sheet. Separate heating circuits were used for the adaptors housing the end windows, to prevent condensation.

Spectra were recorded by means of the Hilger *HF3* hydrogen arc, and iron arc reference spectra were photographed as usual. Control of room temperature was finally achieved to ± 0.2 °C, and high quality spectra were then obtained with cell temperatures up to 90 °C. The vapour pressure of naphthalene at this temperature is 13 mm.

Measurements of the low-dispersion plates were eventually made from $10\times$ enlargements, after it was shown that printing the spectra on hard bromide paper made structure readable that could not be observed conveniently in any other way. The enlargements were made on a grade 5 paper, a mask being used to allow the iron spectrum and the naphthalene spectrum to be exposed independently. Wavelengths were measured from iron lines on the prints; quadratic interpolation gave wavelengths, on measurements of other sharp iron lines, to better than 0.03 Å. Measurements of the less sharp molecular band heads varied by as much as 0.07 Å, or about 0.8 cm^{-1} . In general the low-dispersion measurements of the principal heads were accurate to $\pm 1\text{ cm}^{-1}$ although intervals between heads of similar shape are somewhat more precise.

Spectra photographed in the Ebert spectrograph were taken using a White multiple reflexion cell 80 in. long made of thick Pyrex glass tubing of 2 in. bore. Its volume was about 4 l. One end was closed by a silica window held against a silicone rubber gasket by the flanged tube-end, and the other had a brass end-plate grooved to take a silicone rubber O-ring. An Evans vacuum rotary shaft, the end of which was ground into a screwdriver, was let into the brass plate. This was used to set the number of traversals without affecting the vacuum inside the cell. The White mirrors were of radius of curvature 73.6 in. and the cell was usable up to 28 traversals, giving a path of 52.5 m at 3000 Å before reflexion losses made exposure times too long. By varying the path length all except the temperature-dependent bands could be photographed at room temperature. For these hot bands the cell was fitted with helically wound heating tape and insulated with asbestos wool; thermometers and thermocouples were put close to the cell and windows. The cell was successfully used up to 94 °C. From an initial pressure of 0.1 mm at the start of a series of runs, the pressure in the cell rose at the rate of 0.5 mm

in 24 h. Exposures up to 12 h were required, with xenon arc source. Slit widths were 0.05 mm for the naphthalene bands, and 0.025 mm for the iron arc spectrum.

The wavelengths of the band heads, or intensity maxima, were determined by standard procedures from measurements of the plates made by travelling microscope. The frequencies measured in this way are accurate to $\pm 0.05 \text{ cm}^{-1}$. Some very weak heads had to be measured from prints and are accurate to $\pm 0.1 \text{ cm}^{-1}$. These are indicated in the values listed.

About 1300 band heads or intensity maxima were measured under high dispersion. In the first stage of their analysis, the frequencies were split into blocks of about 100 belonging as far as possible to heads in structurally isolated spectral regions. Complete tables (Vaidya diagrams) of frequency differences were drawn up on an electronic computer and recurrent differences identified. Differences between heads in different blocks were found through a few absorption heads common to the two blocks. This systematic search for common frequency differences greatly helped the subsequent stages of analysis and assignment, and should have brought to light all of the regularities present in the vibrational structure.

RESULTS

The spectrum under low dispersion consists of a number of band groups, each of which is of similar though not identical vibrational substructure. Each band group consists of a principal band and associated sequence bands; two sequences, one of about 10 cm^{-1} and one of about 55 cm^{-1} , appear prominently with up to four or even five members under the conditions used, and there are several other difference bands all weakly developed relatively to them. Figure, 1, plate 9, illustrates three such band groups near the origin, which are of special importance.

The band group on the right of figure 1 is the strongest group of the system, and, in combination with band groups separated from it by totally symmetrical frequencies, accounts for most of the intensity. A large part of the remainder is in band groups similarly related to that at $0+911 \text{ cm}^{-1}$, and a small fraction only in the origin band group, its combinations with totally symmetrical vibrations, and in other very weak bands. It is therefore true in the vapour spectrum, just as McClure showed in the mixed crystal of naphthalene-durene, that the system consists of three interpenetrating sets of bands, namely, the origin band groups, the $0+438$ band group, and the $0+911$ band group, each accompanied by progressions in totally symmetrical vibrations.

The frequency measurements on which the assignments are based are the values measured at high dispersion which agreed throughout with the low-dispersion results to within the accuracy available. The latter are not therefore reported. By selecting the principal head from each band group, that is by discarding all members of known sequences, we get a short list of band heads for assignment. Such a list is given in table 2, together with the proposed assignment and an indication of relative intensity. The bracketed numbers after the head designation are the head separations of doubled bands, to be described below. The frequency differences observed in sequences and difference bands, are, in order of decreasing intensity of the repeated bands, 10, 55, 6, 64, 73, 93 and 133 cm^{-1} .

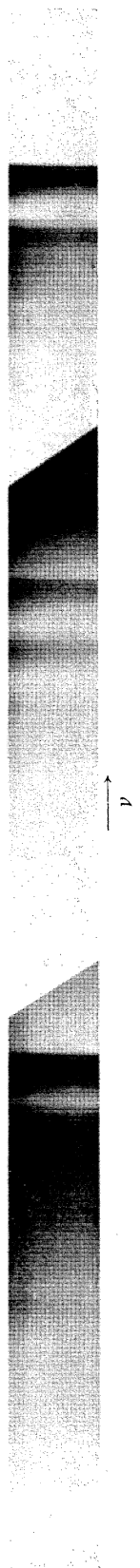


FIGURE 1. Composite enlargement of the spectrum of a part of the 3200 Å naphthalene system from photographs taken with the Hilger large quartz spectrograph. The bands are (right) the $1 \leftarrow 0$ band group $0 + 438 \text{ cm}^{-1}$, the ten times weaker $0 \leftarrow 0$ group (centre) at 32020 cm^{-1} , and the $0 \leftarrow 1$ band group $0 - 506 \text{ cm}^{-1}$ of about the same intensity as the $0 \leftarrow 0$. Individual bands are degraded to the red; and all the sequences strong enough to be seen are also degraded to the red, showing that the high-frequency band is always the principal band of the group, i.e. the first sequence member. The 10 and 55 cm^{-1} sequences are clearly visible in the spectrum.

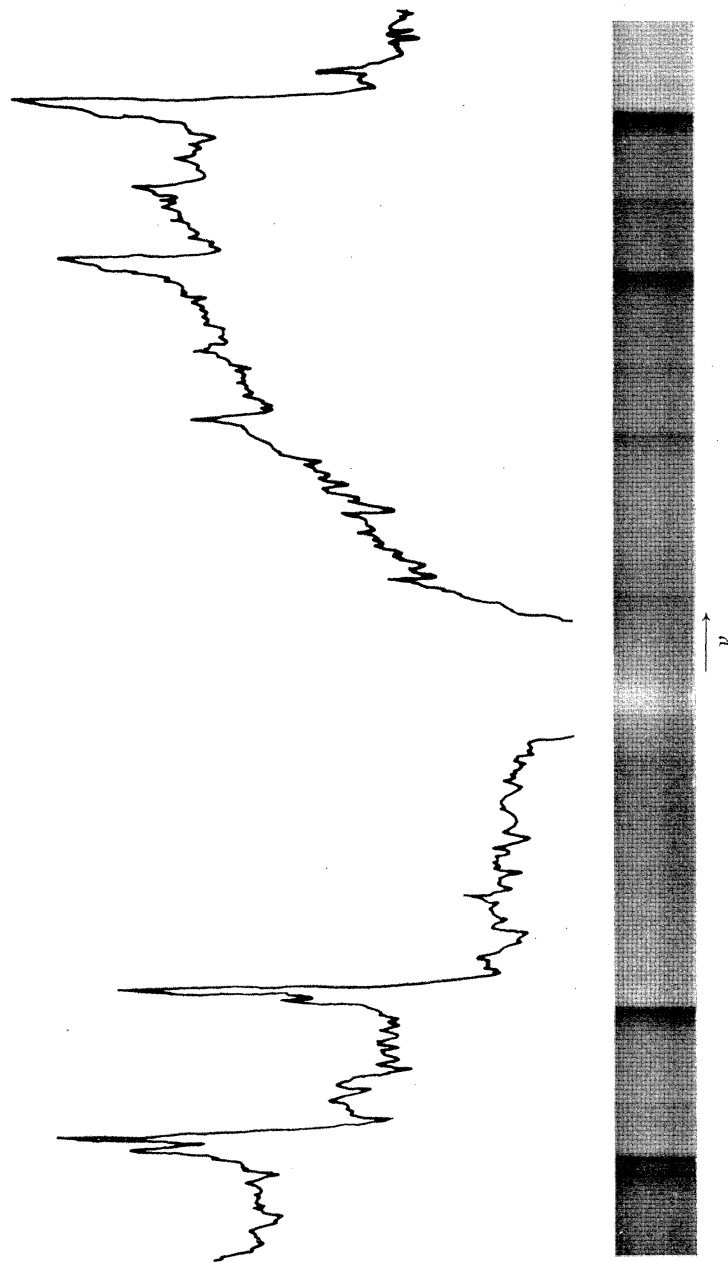


FIGURE 2. High-resolution photograph and microphotometer trace of part of the $0-0$ band group near 32020 cm^{-1} . Several members of the 10 cm^{-1} sequence and one of the 55 cm^{-1} sequence are shown, each with the characteristic single head. The weaker bands lying between the main bands are $\nu'' - \nu'$ bands of about 5 cm^{-1} spacing. The band contours correspond to quasi-parallel A -type bands of an asymmetric rotor.

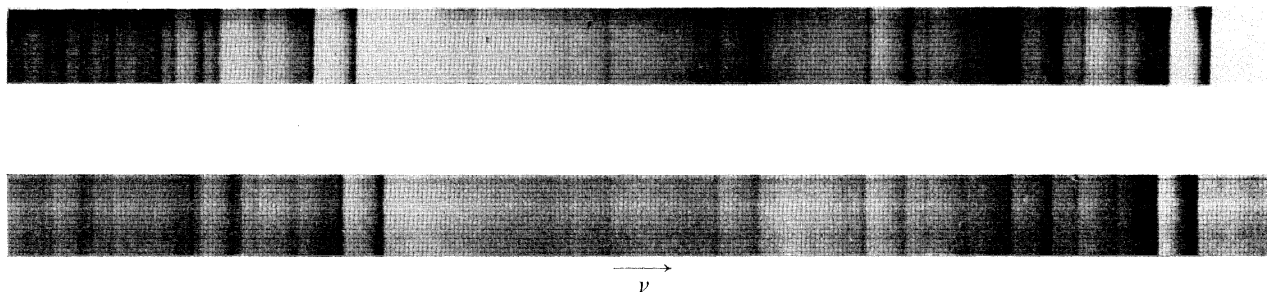


FIGURE 3. High-resolution spectra of parts of the $1 \leftarrow 0$ band group $0 + 438$ near 32458 cm^{-1} (top), and of the structurally similar $0 + 911$ near 32393 cm^{-1} (bottom). The characteristic double maxima of the bands are separated by $2.7\text{--}2.8 \text{ cm}^{-1}$. The contours are those of quasi-perpendicular B -type bands of an asymmetric-rotor.

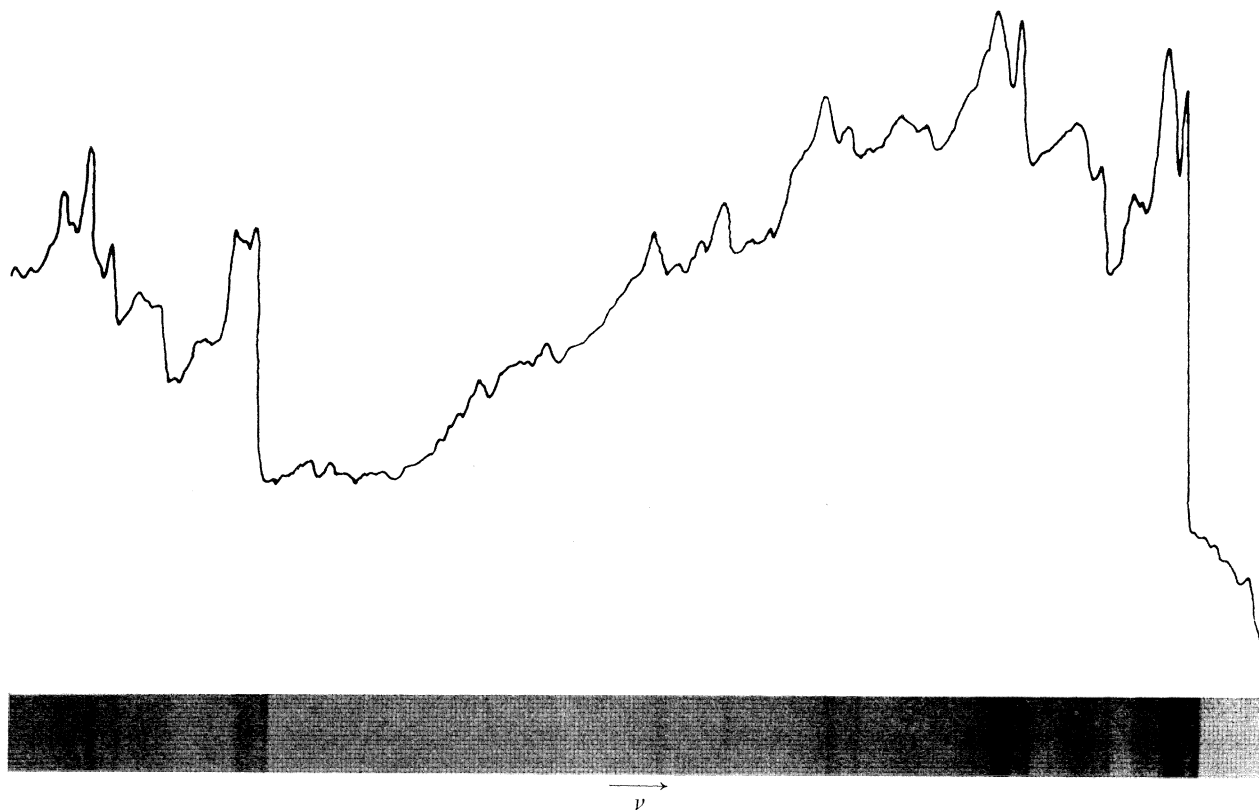


FIGURE 4. Part of the $0 \leftarrow 1$ band group $0 - 506 \text{ cm}^{-1}$ near 31514 cm^{-1} , showing the unique perturbed double-headed band contour found only in this band group.

NAPHTHALENE VAPOUR ABSORPTION BANDS AT 3200 Å. I 547

TABLE 2. PRINCIPAL BAND HEADS: FREQUENCIES (CM⁻¹) AND ASSIGNMENTS

head designation and splitting*	frequency	separation from 0-0	int.†	assignment	Δ
<i>b</i> (3·2)	31 084·0	936·2	vw	0 - 936·2	—
<i>c</i> ‡	31 182·6	837·6	vvw	—	—
<i>b</i> ‡	31 250·4	769·8	vvw	0 - 2 × 385	—
<i>a</i>	31 259·5	760·7	vw	0 - 760·7	—
<i>a</i> (~1·8)	31 514·1	506·1	m	0 - 506·1	—
<i>A</i>	32 020·2	—	m	origin	—
<i>Φ</i> (2·8)	32 226·9	206·7	vvw	—	—
<i>A</i> (2·7)	32 457·9	437·7	vs	0 + 437·7	—
<i>B</i> ‡	32 508·9	488·7	w	—	—
<i>C</i>	32 520·9	500·7	mw	0 + 500·7	—
<i>D</i> ‡	32 561·6	541·4	vvw	—	—
<i>E</i>	32 722·2	702·0	w	0 + 702·0	—
<i>B</i> (2·8)	32 931·2	911·0	ms	0 + 911·0	—
<i>C</i> ‡ (2·9)	32 958·2	938·0	vvw	0 + 437·7 + 500·7	+0·4
<i>F</i>	33 007·6	987·4	vw	0 + 987·4	—
<i>D</i> ‡ (2·7)	33 127·2	1 107·0	vw	—	—
<i>E</i> (2·7)	33 158·5	1 138·3	ms	0 + 437·7 + 702	+1·4
<i>G</i> ‡	33 167·6	1 147·4	vw	0 + 1 147·4	—
<i>F</i> ‡ (2·7)	33 189·8	1 169·6	vw	—	—
<i>H</i> ‡	33 212·2	1 192·0	vvw	0 + 488·7 + 702·0	-1·3
<i>G</i> ‡ (2·8)	33 220·6	1 200·4	vvw	—	—
<i>I</i>	33 344·8	1 324·6	vvw	—	—
<i>K</i>	33 409·7	1 389·5	w	0 + 1 389·5	—
<i>I</i> (2·7)	33 445·4	1 425·2	m	0 + 437·7 + 987·4	-0·1
<i>L</i>	33 454·9	1 434·7	mw	0 + 1 434·7	—
<i>M</i> ‡	33 496·0	1 475·8	vvw	0 + 488·7 + 987·4	+0·3
<i>N</i>	33 508·0	1 487·8	vw	0 + 500·7 + 987·4	+0·3
<i>J</i> (2·6)	33 626·9	1 606·7	vw	—	—
<i>K</i> ‡ (2·9)	33 638·3	1 618·1	vw	0 + 702·0 + 911·0	—
<i>L</i> ‡ (2·9)	33 640·4	1 620·2	vw	0 + 500·7 + 1 107·0	—
<i>M</i> (2·7)	33 658·8	1 638·6	vw	0 + 437·7 + 500·7 + 702·0	+1·8
<i>O</i>	33 735·6	1 715·4	vvw	—	—
<i>N</i> (2·6)	33 869·2	1 849·0	mw	0 + 1 849	—
<i>O</i> (2·8)	33 892·2	1 872·0	mw	0 + 437·7 + 1 434·7	+0·4
<i>P</i> (2·6)	33 918·2	1 898·0	w	0 + 911·0 + 987·4	+0·4
<i>P</i> ‡	33 943·0	1 922·8	vw	0 + 488·7 + 1 434·7	-0·6
<i>Q</i>	33 954·8	1 934·6	w	0 + 500·7 + 1 434·7	+0·8
<i>Q</i> ‡ (2·7)	33 976·7	1 956·5	vvw	—	—
<i>R</i>	33 994·7	1 974·5	vvw	0 + 2 × 987·4	+0·3
<i>S</i> ‡	34 143·8	2 123·6	vw	—	—
<i>R</i> (2·8)	34 146·0	2 125·8	vw	0 + 437·7 + 702·0 + 987·4	+1·3
<i>S</i> ‡ (2·5)	34 176·5	2 156·3	vvw	0 + 987·4 + 1 169·6	+0·8
<i>T</i> ‡	34 225·1	2 204·9	vvw	—	—
<i>U</i> (2·5)	34 322·3	2 302·1	vvw	0 + 911·0 + 1 389·5	-1·5
<i>U</i>	34 341·7	2 321·5	vw	—	—
<i>V</i> (2·7)	34 365·0	2 344·8	vw	0 + 911·0 + 1 434·7	+0·9
<i>V</i>	34 396·1	2 375·9	vw	0 + 987·4 + 1 389·5	+1·0
<i>W</i> (2·6)	34 432·4	2 412·2	vw	0 + 437·7 + 2 × 987·4	+0·5
<i>W</i>	34 441·2	2 421·0	vw	0 + 987·4 + 1 434·7	+1·1
<i>X</i> (2·7)	34 592·0	2 571·8	vvw	0 + 437·7 + 702·0 + 1 434·7	+2·6
<i>Y</i> ‡ (2·5)	34 623·7	2 603·5	vvw	0 + 1 169·6 + 1 434·7	+0·8
<i>Z</i> (2·5)	34 625·0	2 604·8	vvw	0 + 2 × 702·0 + 1 200·4	-0·5
<i>Δ</i>	34 655·5	2 635·3	vvw	—	—
<i>Γ</i> (2·9)	34 831·8	2 811·6	vvw	0 + 437·7 + 987·4 + 1 389·5	+3·0
<i>Π</i>	34 842·0	2 821·8	vw	0 + 2 321·5 + 500·7	+0·4
<i>Δ</i> (2·7)	34 856·2	2 836·0	vvw	0 + 1 849·0 + 987·5	+0·5
<i>Λ</i>	34 885·7	2 865·5	vw	0 + 2 × 1 434·7	+3·9
<i>Π</i> ‡ (2·7)	34 905·0	2 884·8	vvw	0 + 911·0 + 2 × 987·4	+1·0
<i>Δ</i> (2·6)	35 086·9	3 066·7	vw	—	—

* Single-headed bands are denoted by Roman letters, double-headed bands by italics.

† Intensities are estimates from the appearance of the bands; the estimates depend somewhat on the background, which increases to shorter wavelength.

‡ Seen at high resolution only.

In the low-dispersion photographs the bands showed a striking difference in head structure. Those of the 0–0 group had sharp single heads, but in the 0+438 group the intensity maxima were clearly doubled, with a separation in the range 1 to 3 cm⁻¹. The heads in the 0–506 group seemed too broad to be single, but were not then resolvable. All other band groups could be definitely assigned to one or other class, namely, single or double headed. The head structure was the feature that prompted a study of the system under high resolution, in the expectation that the rotational contours of the bands might be sufficiently well resolved to permit some use to be made of them in the analysis. Some key regions of the high-resolution spectra are shown in figures 2, 3 and 4. Figure 2, plate 9, shows several members of the 10 cm⁻¹ sequence of the 0–0 band at 32 020 cm⁻¹, which is a typical single-headed band group.

Figures 3 and 4, plate 10, similarly apply to the 1 ← 0 band 0+438 and the 0 ← 1 band 0–506, respectively. The 0–506 band group is exceptional; the 0–0 and 1–0 bands illustrated show the types to which, one or other, all the band groups of the spectrum conform. The differences that occur concern only the head spacing of double-headed bands, which varies a little from case to case, as shown in table 2 by the bracketed numbers following the head designation.

A complete list of band heads measured, and their assignments where known, are given in appendix 1.

DISCUSSION

The band contours

The most important single feature of the band system under high resolution is the clear division of the bands into two types, distinguished by their contours as shown in figures 2, 3 and 4. Band contours are characteristic of the polarization directions of the transition, and have been widely employed to assign transitions of smaller and simpler molecules. Their use for larger asymmetric top molecules such as naphthalene is, so far as we are aware, novel; but it seems to be a promising method of assigning transitions when the two conditions are satisfied that the bands can be adequately resolved, and the dimensions of the combining electronic states are known closely enough to enable the calculation of expected contour types, as will now be described.

Naphthalene is an asymmetric top for which the three reciprocal moments of inertia in the ground state may be found from the molecular structure determined in the crystal (Abrahams, Robertson & White 1949). The C—H distances were taken equal to those in benzene, namely 1.08 Å. The values are $A = 0.103$ cm⁻¹, $B = 0.0422$ cm⁻¹ and $C = 0.0302$ cm⁻¹. The inertial axes are, in order, the short in-plane axis, the long in-plane axis and the normal. These values imply an asymmetry parameter $\kappa = -0.67$. Small changes of dimensions within the limits of precision of the structural measurements give $\kappa = -0.67$ to -0.68 . If the upper-state dimensions are the same, the calculations of Dennison (1931) (see also Herzberg 1945) show that type *A* bands are recognizably similar to parallel bands of a symmetric top, showing a strong central *Q* branch and weaker *P* and *R* branches. Type *B* bands on the other hand have an intensity minimum at the band origin, flanked by two sets of lines forming two equi-distant intensity maxima. Type *C* bands are not sufficiently different from type *B* for these values of κ to enable an easy distinction to be drawn. The observed naphthalene bands conform generally to these

NAPHTHALENE VAPOUR ABSORPTION BANDS AT 3200 Å. I 549

descriptions of type *A* (quasi-parallel) single-headed bands and type *B* or *C* (quasi-perpendicular) double-headed* bands. Accordingly, it seemed probable that the single-headed bands were long-axis polarized, and the double-headed bands short-axis polarized. The possibility that the double-headed bands are *C*-type polarized normal to the molecular plane is incompatible with a transition between π -electron states and will not be further considered. Band contours of types corresponding to unchanged κ have been observed in the infra-red spectrum of naphthalene by Person, Pimentel & Schnepf (1955), and similarly interpreted.

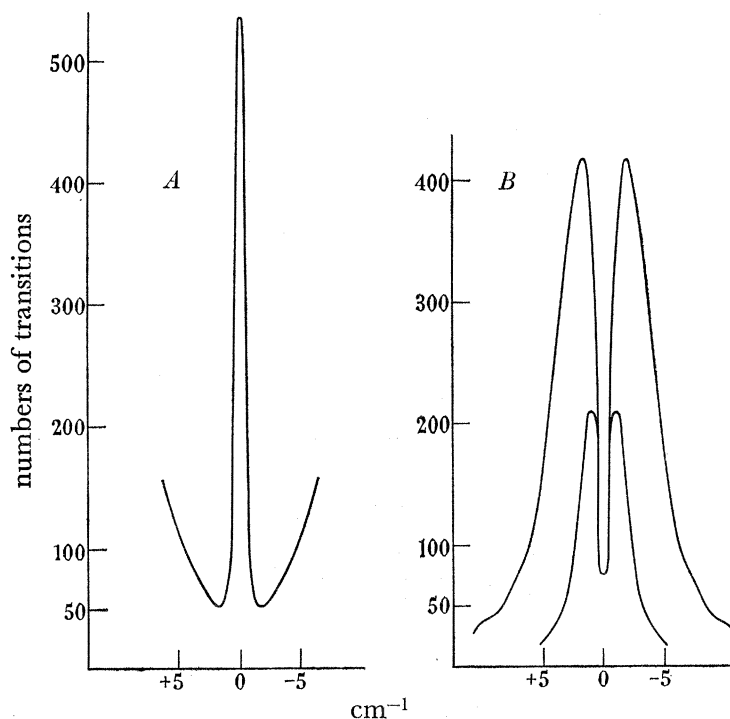


FIGURE 5. Contours of type *A* and *B* bands for equal upper and lower asymmetry, $\kappa = -0.68$. Contours record transitions per unit frequency as a function of displacement from the band origin. The lower curve for *B* bands includes transitions up to $J = 20$; the upper curve up to $J = 40$.

The formation of heads accompanied by degradation towards the red in our spectra is due to a change of rotational constants in the upper state, and further work was required to explore the effect on the contours of changes in the upper-state values, and to extend Dennison's calculations for unchanged κ to J values higher than his limit of $J = 4$. Accordingly, computer programs were developed to calculate the levels of the asymmetric rotor.†

Calculations were made in the first instance of transitions $\Delta K = 0, \pm 1$, up to $J = 20$ for equal upper- and lower-state asymmetry, namely $\kappa = -0.68$ and for type *A* and *B* bands. Intensities have not been calculated, and the results in figure 5 are a plot of the number of lines per unit frequency interval against frequency.

* Strictly, it is not certain that the longer wavelength peak is truly a head, or simply a sharp maximum.

† Calculations up to $J = 20$ were programmed for the I.B.M. 650 computer by iteration on the continued fraction as described by King, Hainer & Cross (1943) with convergence improvement by Posener's method (1956). Subsequently, calculations up to $J = 40$ were made on the I.B.M. 704 computer by matrix diagonalization.

The *A*-band contour shows the prominent *Q*-type branch giving the central maximum found by Dennison and two weaker satellite branches. The *B*-band contour has two equal maxima equally displaced from a central minimum at the band origin and separated by 2.1 cm^{-1} . Figure 5 includes also the results of calculations including transitions up to $J = 40$. In the *A*-band contour the added transitions build up the central peak into an intense narrow band maximum and extend the wings; in the *B* band the new lines mainly build on to the outer zones of the two maxima, and widen the gap between them to about 3.5 cm^{-1} . This increase of head spacing is exaggerated because we have not included the weakening of the line intensities by the Boltzmann factor, which becomes significant between $J = 20$ and $J = 40$, and will reduce the widening of the spacing of the maxima due to lines of higher J . The spacing found in the spectrum varies between 2 and 3 cm^{-1} and, at least for some of the bands, the calculated contours for equal asymmetries give an acceptable fit. In general the observed *B*-type bands show a splitting between the values calculated for $J = 20$ and $J = 40$, and are also degraded, showing that some change in rotational constants takes place on electronic excitation. Evidence from the vibrational structure of the band system will be interpreted later in: his paper to show that the dimensional change is small, insufficient in any one normal co-ordinate to produce progressions of more than two members. A number of trial upper-state structures were however considered, and κ values calculated for them. These may be summarized as follows:

(i) Structures in which each ring is a regular hexagon, with C—C bond lengths increased to a value between 1.41 and 1.46 \AA , and C—H bond lengths varied between 1.06 and 1.08 \AA . In an extreme variation of this type, namely, to $r_{\text{C—C}} = 1.46 \text{ \AA}$, $r_{\text{C—H}} = 1.06 \text{ \AA}$ κ changes only to -0.70 from -0.67 or -0.68 in the ground state. In general κ varies little so long as the rings suffer no angle changes.

(ii) Structures in which the ring angles are changed (preserving D_{2h} symmetry) with or without an increase in C—C bond length. Variations of this type give a rapid change in κ ; for example, for equal bond lengths of $r_{\text{C—C}} = 1.43 \text{ \AA}$ and $r_{\text{C—H}} = 1.06 \text{ \AA}$ a 7° decrease of the C—C—C bond angle at the α -carbon atoms, and implied increases elsewhere, corresponding to a compression of the molecule along the long in-plane axis, gives $\kappa = -0.60$. An elongation of the molecule conversely gives a corresponding increase in κ .

To include the range of κ values that seems physically possible, we have computed the contours based on the density of transitions per unit frequency for cases of $\kappa = -0.63$ and $\kappa = -0.81$, for J values up to 40 and for transitions $\Delta K = 0, \pm 1$. The contours for the lower κ value are strongly degraded to the blue; in this and other respects they are incompatible with experiment. The contours for upper state $\kappa = -0.81$ are given in figure 6.

Under this extreme increase in κ both *A*- and *B*-type bands are substantially changed. The *A*-type band contour shows a strong central maximum as before, but now with fairly intense subsidiary maxima separated by 4 cm^{-1} to the high-frequency, and by 2 cm^{-1} to the low-frequency sides. These features are not observed in the naphthalene bands. Likewise the calculated *B*-type bands show features not found in the actual spectrum, notably the development of a substantially greater density of transitions in the low-frequency maximum than in the higher. A substantial intensity difference in the main maxima is a feature which could not have escaped detection in the observed bands, and its absence

NAPHTHALENE VAPOUR ABSORPTION BANDS AT 3200 Å. I 551

suggests that the upper state κ is much nearer to the ground-state value -0.68 than to -0.81 . However, without calculations to include intensities and allowance for Boltzmann factors it is not possible to come to definite conclusions as to the upper state κ : but it seems clear that for any value compatible with the vibrational structure double-headed bands record *B*-type short-axis transitions. Our use of contours is confined for the present

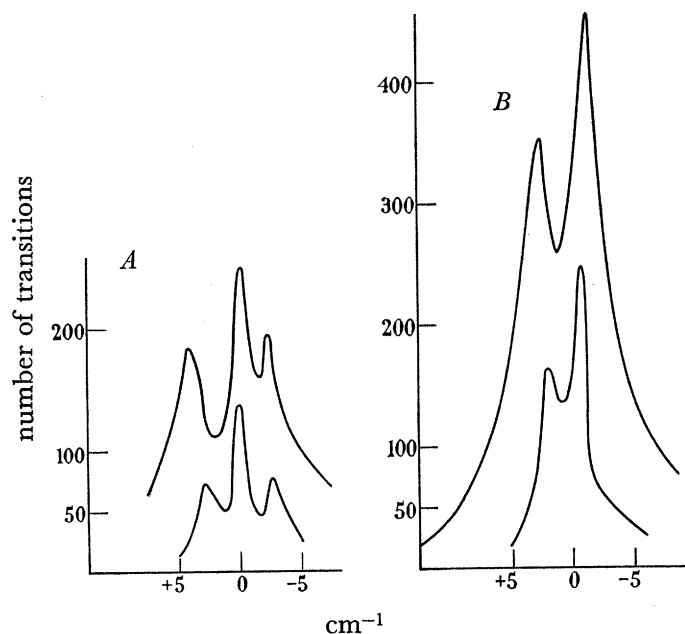


FIGURE 6. Calculated band contours for *A*- and *B*-type bands. Upper state $\kappa = -0.81$, ground state $\kappa = -0.68$. The contours give the density of transition per unit frequency. The lower curve includes transitions up to $J = 20$, the upper curves up to $J = 40$.

to this main point, although it is clear that much information may be accessible from the study of contours and head spacings (which vary considerably) in the several bands. The more intense double-headed bands, including $0-506$, $0+438$ and $0+911$ also show some very weak rotational wings rising to poorly defined maxima. These features are marked as wings in the appendix.

The hot bands

The temperature dependence of the intensity in this system in naphthalene vapour was studied by Knipe *et al.* (1953). Their study disclosed that the band group at 31514 cm^{-1} in the vapour was temperature dependent to a degree suggesting a $0 \leftarrow 1$ transition in a frequency of about 500 cm^{-1} . A similar and more specific conclusion came out of solution intensity experiments by Passerini & Ross (1954), who made an estimate of $544 \pm 60 \text{ cm}^{-1}$ for the excitation of the initial state and suggested that the band group at 32020.2 cm^{-1} (our value) was the $0-0$ group of the system. McClure confirmed this, and additional confirmation can be found in our work.

In the first place measurements of the temperature dependence of intensity showed that the 32020 cm^{-1} band group has a vibrationally unexcited ground state. Also it was shown that band groups to the red of the group at 31514 cm^{-1} depend more strongly on temperature than does 31514 cm^{-1} itself, that is, their initial states are more vibrationally excited than the 500 cm^{-1} excitation of the 31514 cm^{-1} group. Moreover, a careful search

showed no principal bands to the red of the supposed origin at 32020 cm^{-1} that are temperature independent; and an analysis of the frequency intervals between 32020 cm^{-1} and the hot bands discloses in some cases agreement with recognized ground-state vibrations. The band at 31259.5 cm^{-1} is 761 cm^{-1} to the red of the origin band, corresponding to the strong polarized Raman frequency variously reported between 758 and 763 cm^{-1} (see, for example, Brandmuller & Schmid 1956). Both the origin and $0-761$ bands have the same single-headed rotational contours, a fact which agrees with the totally symmetrical assignment of the 761 cm^{-1} vibration. The interval 936 cm^{-1} between the origin and the principal band at 31084 cm^{-1} is also close to a Raman interval. The Raman line is, however, weak and its frequency not closely determined. Braun, Spooner & Fenske (1950), Luther & Hampel (1950) and Lippincott & O'Reilly (1955) report 944 , 941 and 941 cm^{-1} , respectively, from studies of molten naphthalene; Luther & Hampel quote 938 cm^{-1} as the mean of values in the earlier literature. The frequency has either been disregarded as a fundamental or assigned to the totally symmetrical species a_g on the depolarization factor of 0.63 obtained by Braun *et al.* However, this value, obtained on so weak a line, cannot be regarded as decisive. In our spectra the band $0-936$ is clearly of the double-headed class and therefore of opposite polarization to the $0-0$ band; we can therefore assign the frequency 936 cm^{-1} to the in-plane non-totally symmetrical species b_{3g} .

The most intense of the hot bands is at 31514 cm^{-1} displaced by 506 cm^{-1} from the origin. This band is the hot analogue of the strong band at 32458 cm^{-1} , and is itself observed as the strongest false origin of the fluorescence. Previous interpretations of the spectrum have been based in part on identifying this frequency with the very strong Raman displacement of 512 cm^{-1} , and this is the root-cause of the inconsistencies which have arisen in the proposed analyses of the u.v. spectra. It is not compatible with our observations to suppose that the Raman 512 cm^{-1} appears in this way. In the first place the interval is close to 506.0 cm^{-1} measured from the single head of the $0-0$ band to the short wave member of the double head of $0-506$. Between band origins the separation is probably very close to 507 cm^{-1} . Measurements of the Raman displacement, however, cluster closely round the value 512 cm^{-1} , with slightly higher values of about 514 cm^{-1} for the melt (Kohlrausch 1943, Luther 1948, Stein *et al.* 1952, Brandmuller 1953). In a recent report Mitra & Bernstein (1959) also favour the value 512 cm^{-1} . These facts made plausible the idea that there are two fundamentals near 500 cm^{-1} and not one. Confirmation is found in the rotational contour illustrated in figure 4, which shows that $0-506$ is a double-headed band. It follows that the interval corresponds to a new non-totally symmetrical vibration. We assign it to the species b_{3g} . The strongly Raman active a_g frequency usually quoted as 512 cm^{-1} cannot be identified with certainty in our spectra. It is the ground-state analogue of the a_g 501 cm^{-1} in the upper state, and might therefore be expected only to be as weakly active, singly or in combinations, as 501 cm^{-1} is in the upper state. We should thus only expect to observe it in combination with intense double-headed origins, for example, in $0-512+438$, $0-512+911$ and $0-512-506$. The first two combinations are under much stronger bands and are not observed. However, in both low and high resolution plates a very weak and poorly resolved hot band appears at 30996 cm^{-1} . Two assignments seem plausible: $0-506-516$ and $0-936-87$, the

frequency difference 87 being a sequence interval somewhat doubtfully identified in a small number of other bands. The latter assignment is unlikely to be correct, because the doubtful 87 cm^{-1} sequence, where it is thought to appear, carries only a minute fraction of the principal band's intensity, and probably would not be observable in this case. There is another reason for preferring the first assignment, which is that in McClure's mixed crystal fluorescence measurements a band with short axis polarization appeared at $0-1024\text{ cm}^{-1}$, which seems to correspond to the vapour band at 30996 cm^{-1} . Since McClure's spectrum was measured at $20\text{ }^\circ\text{K}$ it includes no sequence bands, and the assignment $0-509-516$ is therefore the likely one. If correct, the indicated ground-state frequency in the vapour is 515 to 516 cm^{-1} instead of the 512 cm^{-1} obtained by averaging the literature values of the Raman displacement. Clearly, however, the frequency is not well established in the absorption spectrum; no other expected combinations of it could be found. The value 517 cm^{-1} has also recently been found by Bolotnikova (1959) from measurements of the fluorescence of naphthalene in durene crystals, and in solution in pentane, both at $77\text{ }^\circ\text{K}$.

The vibrational structure to the red of the $0-0$ band can thus be described as involving two false origins, each differing from the true electronic origin by a non-totally symmetrical frequency, one 506 cm^{-1} and the other 936 cm^{-1} . This agrees closely with the situation on the high-frequency side of the $0-0$ band, as will be shown, and there is a good 'mirror symmetry' between the activity of upper-state vibrations in combination with the electronic ground state and ground-state vibrations in combination with the pure electronic upper state, in so far as these can be observed. To summarize, we give in table 3 the inferences about ground-state frequencies made, or supported, by the study of hot bands. The upper-state analogues are shown in brackets.

TABLE 3. LOW GROUND-STATE FREQUENCIES OF NAPHTHALENE (CM^{-1})

species a_g	species b_{3g}
516 (501)	506 (438)
761 (702)	936 (911)

A reasonable further inference is that there is no lower-frequency vibration of class b_{3g} than 506 cm^{-1} because, if there were, it would be expected to show itself in further double-headed bands lying between the origin and $0-506$ in a spectral region clear of other absorption. In particular, the Raman frequency 385 cm^{-1} must belong to one of the out-of-plane symmetry classes and not to the in-plane b_{3g} class, as has sometimes been suggested.

Table 2 includes two other intervals (769.8 and 837.6 cm^{-1}) appearing as separations between hot bands and the origin and there are two more (944.3 and 947.4 cm^{-1}) that are doubtful. Both of the better resolved intervals appear separating single-headed bands and are therefore totally symmetrical fundamentals or combinations. 769.8 cm^{-1} may be associated with a frequently reported weak Raman line recently given by Luther, Feldman & Hampel (1955) at 774 cm^{-1} in CS_2 solution. It does not seem likely that either of 769.8 and 837.6 are new totally symmetrical frequencies. The first may be interpreted as two quanta of the weak Raman fundamental of about 385 cm^{-1} belonging to an out-of-plane g species (Lipincott & O'Reilly 1955); the second we cannot explain at present.

Combinations of a ground-state frequency with an upper-state frequency have not been observed, although there are several that might have been expected under the conditions used. For example, the combinations $0+501$ and $0-506+501$ should be of comparable intensity, because the bands $0-0$ and $0-506$ are themselves comparable. The latter combination could not be detected, however, and must be masked by the much stronger adjacent origin band. Some other combinations are similarly masked, but others such as $0-506+1435$ fall in relatively empty spectral regions and may be detectable under different conditions, notably higher temperatures, than have been used. Combination bands of similar type do occur in the emission spectrum of naphthalene induced by radio-frequency discharge, notably $0-506+702$ and $0+438-760$ (Freeman 1959; Guilbert 1955; S. J. Leach & J. Guilbert, private communication).

The double-headed band $0-506$ is unique in the spectrum in the character of its low-frequency maximum. All other double-headed bands show two sharp intensity maxima, separated by a gap in which there is, in the stronger bands, a very weak rotational wing and in the weaker bands no absorption visible at all. The $0-506$ band and its sequence bands have a sharp high-frequency head, and a second broad maximum about 1 cm^{-1} wide, running out to 1.8 cm^{-1} from the head. Thus the band structure is related to the normal double-headed bands by what appears to be a reduction of the head spacing and a marked intensification of the rotational wing to a point where it merges with the normal low-frequency head.

We cannot offer a detailed explanation of the rotational perturbation causing this marked change in the band shape. It seems plausible, and fits the known facts, to suggest that it is due to the closeness of the two fundamentals 506 and 516 and their coupling by the Coriolis force. These fundamentals differ by a symmetry component b_{3g} and may interact with one another under a rotation about the inertial axis normal to the molecular plane. The interaction, as is well-known, increases quadratically with J and inversely with the separation between the interacting levels. Superficially there is nothing against the idea that in the observed bands the perturbation consists of the displacement of the rotational lines belonging to high J quantum numbers to slightly higher frequency (because the perturbing level $0-516$ is at lower frequency). There is some confirmation in the fact that in octadeuteronaphthalene where the interacting vibrations are even closer in frequency the perturbation is much more severe. A search for other cases in the naphthalene spectrum where Coriolis coupling might be looked for shows that the conditions near 506 to 516 cm^{-1} are indeed unique, and that no similar adjacent pair of fundamentals occurs of the right symmetry, and of which at least one is spectrally active.

Vibrational structure: progressions

The analysis we shall give is based on a vibrational structure consisting in the main of three interpenetrating sets of band groups; one set originates on the $0-0$ group and its progressions, another on a five or ten times stronger false origin at $0+438$, and a third on a false origin at $0+911$, giving a somewhat weaker set of bands. Bands which show the same single-headed band contours as the origin band (see table 2) differ from it by a totally symmetrical frequency or combination of frequencies. We thus identify the following definite totally symmetrical upper-state fundamentals: 501 , 702 , 987 , 1390 , 1435 . Each

NAPHTHALENE VAPOUR ABSORPTION BANDS AT 3200 Å. I 555

of these, with one exception where a coincidence makes it unobservable, appears in combination also with the false origins $0+438$ and $0+911$, and again give bands with the same (double-headed) contour type. A striking feature of the vibrational structure is that only in a few cases is a two-quantum interval in any of these frequencies observed, and the exceptions $0+2\times 987$, $0+438+2\times 987$ and $0+2\times 1435$ are weak. There are thus probably no progressions with significant intensity in more than one or two members, and in all cases the one-quantum addition gives a band weaker than the principal band. This greatly simplifies the vibrational structure. Interpretation of this fact involves the Franck–Condon principle, and is that the changes in dimensions of the molecule on electronic excitation are small compared with the amplitudes of vibrations in the totally symmetrical frequencies. Methods like those used to deal with the structure of the benzene 2600 Å system (Craig 1950) suggest an upper limit of 0.015 Å for the displacement of any C atom *in any one normal mode*. In general, such changes as do occur must be supposed to affect several of the totally symmetrical normal co-ordinates, and the resultant displacement of the nuclear framework is the combined one due to all those changed. It is not possible to use the Franck–Condon principle to get a precise estimate of the change of size on excitation because the form of normal co-ordinates is not known, but we think it unlikely from the spectral evidence that any C atom is displaced from its ground-state position by more than 0.01 to 0.02 Å. Another important conclusion concerns a possible change of molecular symmetry upon excitation. It is well known that a change of symmetry manifests itself by the appearance of progressions in vibrations which, with respect to the covering symmetry of the ground state, are non-totally symmetrical. No such progressions have been found, despite the fact that naphthalene has low-frequency vibrations in all the symmetry species which would have been readily detected in hot bands. We may conclude that naphthalene belongs to the planar D_{2h} symmetry group in the excited electronic state as in the ground state, and that its dimensions are little changed on excitation.

Bands originating at the electronic origin

One of the three sets of interpenetrating band groups in the system is the set of single-headed long-axis polarized bands corresponding to the pure electronic transition. The strongest is the origin band itself. In solution spectra this band is between one-tenth and one-fifth as strong as the vibration induced band $0+438$ and the same intensity ratio appears compatible with the appearance of the vapour spectrum, in which overlapping prevents an acceptable independent measurement of intensity. However, the origin band is stronger than the Boltzmann-weakened $0-506$ (Boltzmann factor one-twelfth at 20 °C) at room temperature though very much weaker than $0+438$, and since the intrinsic strength of $0-506$ and $0+438$ should be nearly the same we have a rough confirmation of the intensity ratio between the allowed and induced band. The total oscillator strength of the system measured in solution is $f \simeq 0.002$, and that of the electronically allowed bands about $f \simeq 0.0002-0.0004$. The frequency of the electronic origin in the vapour is $32020.16 \pm 0.05 \text{ cm}^{-1}$.

Bands originating at the false origin $0+438 \text{ cm}^{-1}$

The band group $0+438$ starting at 32459.5 cm^{-1} and illustrated in figure 3 is the strongest of the system and, with its combination bands, provides most of the intensity.

The interval 438 cm^{-1} separates two bands of different contour type; and must therefore represent a non-totally symmetrical fundamental or combination of species b_{3g} , analogous to the ground state 506 cm^{-1} b_{3g} fundamental. According to the calculated contour the band origin lies midway between the two maxima; the measured frequencies refer to the high-frequency maximum, so that, calculated for band origins, the true frequency is near 437 cm^{-1} . We shall, however, refer throughout to measurements of the high-frequency maximum.

Bands originating at the false origin $0+911\text{ cm}^{-1}$

These bands form a subsidiary vibration-induced set weaker than those induced by the 438 cm^{-1} vibration but generally similar in appearance to them. The principal band and its 10 cm^{-1} and 55 cm^{-1} sequences are shown in figure 3.

The bands originating in $0+911\text{ cm}^{-1}$ show a striking resemblance in contour and in associated progressions to the $0+438\text{ cm}^{-1}$ set. The band $0+911+501$ is not observed, presumably because it underlies the much stronger combination $0+438+987$, but with this exception the two sets of band groups show the same progression intervals. Thus 911 cm^{-1} is accepted as the upper state b_{3g} fundamental analogous to 936 cm^{-1} in the ground state; its perturbing power for the electronic transition is similar to, but weaker than, that of the b_{3g} upper state vibration of 438 cm^{-1} .

Occurrence of sequences: ground-state vibrations

The occurrence of sequences depends primarily on the population of the vibrationally excited initial state, low-vibrational frequencies being associated with long sequences, and higher frequencies with sequences consisting of one repetition band only, or not appearing at all. In the naphthalene spectrum there are long sequences in 10 and 55 cm^{-1} intervals and several other sequences of which only one interval is observed. Whether or not the members of a particular sequence are observed depends not only on the Boltzmann factor, but also on the presence of other stronger bands that may overlies a particular member. Near coincidences of this sort do occur in naphthalene. For example, the second sequence member in 64 cm^{-1} would be obscured by the very much more intense sequence band $2\times 55+2\times 10$. However, it remains a striking fact that both 10 and 55 cm^{-1} can be observed in up to 5 intervals, while none of the difference frequencies of 6, 64, 73, 87, 93, 99 and 133 form sequences of more than one member under the conditions of temperature and path length used. The reality of the other intervals and their interpretation as $\nu'' - \nu'$ differences seems well established in all except, perhaps, 87 cm^{-1} . The interval 87 cm^{-1} appears only three times in the measured bands; the others have been observed ten times or more. Their assignment as $\nu'' - \nu'$ differences is indicated because they appear in band groups associated with hot bands as well as with bands originating in the non-vibrating ground state and therefore can have no other general explanation. They are, moreover, not observed in the low temperature solid-state spectra of McClure.

The occurrence of long sequences in 10 and 55 cm^{-1} gives the characteristic appearance to the bands shown in figures 1 to 4. Intervals between successive sequence members in the 10 cm^{-1} sequence are constant within experimental error in the $0-0$, the $0+438$ and the $0+911\text{ cm}^{-1}$ band groups, which are among the best resolved in the system. The 55 cm^{-1} sequences shows a definite convergence, amounting to 0.7 cm^{-1} in the fourth

NAPHTHALENE VAPOUR ABSORPTION BANDS AT 3200 Å. I 557

interval compared with the first. This convergence is about the same in the three band groups mentioned, and is presumably due to a more rapid closing of the levels in the excited state than in the ground state.

The fact that there are just two strongly developed sequences suggests that there are two ground-state frequencies much lower than any others. This conclusion is in general agreement with infra-red and Raman measurements. However, differences between the many published spectra both as to frequencies and to assignments deduced make the situation confused. There seems little doubt that the frequencies 176 and 195 cm^{-1} are compatible with the production of the long sequences in 10 and 55 cm^{-1} , the Boltzmann factors at $290\text{ }^\circ\text{K}$ being, respectively, 0.42 and 0.38 for singly excited vibrations and 0.031 and 0.021 for four-quantum excitations. It is not possible to decide from our spectra which of the two vibrations to associate with each sequence. We think that the 10 cm^{-1} sequence is slightly stronger in its later members, and therefore that the 176 cm^{-1} rather than the 195 cm^{-1} vibration produces it, but this conclusion is uncertain. If correct, the two corresponding frequencies in the upper state are 166 and 140 cm^{-1} .

A third fairly strong sequence would have been expected to appear in the frequency 285 cm^{-1} with Boltzmann factor 0.24 at $290\text{ }^\circ\text{K}$; the Boltzmann factor for two quanta is nearly equal to that for 3×195 , therefore at least two and perhaps three sequence intervals should be seen to match the three or four in 195 cm^{-1} . No sequences except the 10 and 55 cm^{-1} were seen in more than one interval and with the possible exception of the 6 cm^{-1} sequence, do not seem strong enough for a 285 cm^{-1} fundamental. The reality of the frequency 285 cm^{-1} is not put beyond doubt by published work; and our spectra would be more easily explained if the next lowest frequency were 360 cm^{-1} or above, as recently favoured by Luther, Brandes, Gunzler & Hampel (1955). If the 285 cm^{-1} fundamental is real, the sequence associated with it is certainly that in 6 cm^{-1} differences, giving an upper-state value 279 cm^{-1} . The first member of this sequence appears consistently throughout the spectrum, at an interval which varies in the range $4.5\text{--}7\text{ cm}^{-1}$. In examples at the lower end of this range a second member would be obscured by the intense first member of the 10 cm^{-1} sequence. But there are a few band groups in which the difference is higher showing a second band, otherwise unassigned, in about the position of an expected second member. For example, the principal head band at 32520.9 cm^{-1} has a sequence band separated by 5.2 cm^{-1} ; there is an unassigned band at 32510.0 cm^{-1} separated by a further 5.7 cm^{-1} which might be taken to be the second sequence member. However, an *increase* of 0.5 cm^{-1} is unusual in any sequence, and has no parallel in the others in this spectrum. In a second example the principal band head at 32722.2 has a difference band 6.7 cm^{-1} away at 32715.5 ; an otherwise unassigned band at 32708.7 is separated by a further 6.8 cm^{-1} . The second interval would again be greater than the first, but by a much smaller amount than before. The assignment is thus unconvincing. Similar possible second members of the 6 cm^{-1} sequence were examined in a number of the band groups, but were not considered to be established. The spread 4.5 to 7 cm^{-1} for the sequence interval is greater than that found in any of the other sequences, and is a further puzzling feature. In spite of these difficulties, we think that for want of a better alternative the 6 cm^{-1} interval represents a difference frequency. It cannot be due to $\text{C}_{10}\text{H}_7\text{D}$, because deuteration causes a *blue* shift in the spectrum.

Other principal band heads

After sequence bands and progression bands in the totally symmetrical frequencies have been set aside, there remains a small number of the principal bands to be dealt with. Eighteen bands remain including the electronic origin, and the two strong false origins $0+438$ and $0+911$ cm^{-1} . Of the other fifteen, eight are double-headed and therefore vibration induced, and seven are electronically allowed. The double-headed bands include: $0+1107\cdot0$ (vw), $1169\cdot6$ (vw), $1200\cdot4$ (vvw), $1849\cdot0$ (mw), $1956\cdot5$ (vvw), $2604\cdot8$ (vvw) and $3066\cdot7$ (vw). These intervals must represent fundamentals or combinations of symmetry b_{3g} ; not all can be fundamentals since two of the eight of species b_{3g} have already been assigned (438 and 911 cm^{-1}). Thus at least one of the intervals, and we think more than one, must be a combination of a lower b_{3g} fundamental and one or more totally symmetrical frequencies. The intensity of $0+1107\cdot0$, $0+1169\cdot6$, $0+1849\cdot0$ and perhaps $0+1200\cdot4$ suggests that these represent b_{3g} fundamentals. The others are probably combinations of 438 or 911 cm^{-1} with totally symmetrical frequencies which are otherwise unidentified. The set of three double bands displaced from the origin by $1606\cdot7$, $1618\cdot1$ and $1620\cdot2$ cm^{-1} show the most definite example of a vibrational perturbation, in this case Fermi resonance, among the bands measured. The combination $0+702+911\cdot0$ should be comparable in intensity with the weak band $0+911\cdot0+987\cdot4$ because both are built on the false origin $0+911\cdot0$ with totally symmetrical frequencies which, in combination with the other false origin $0+437\cdot7$ give comparably strong bands. Yet there is no band closer than 5 cm^{-1} higher than the calculated $0+1613$ cm^{-1} for the missing combination. On the other hand, the combination $0+500\cdot7+1107\cdot0$ appears unexpectedly strongly 1 cm^{-1} below its calculated position. The presence of a third band together with these perturbations suggests another weakly active b_{3g} fundamental, probably at about 1610 cm^{-1} causing the displacements of the combinations mentioned and itself being displaced to higher frequencies. The frequency 1610 cm^{-1} is not observed in any other bands, and must gain its intensity from the $0+702\cdot0+911\cdot0$ combination in the Fermi resonance. Uncertainty also attaches to the seven totally symmetrical intervals, which are $0+488\cdot7$ (w), $541\cdot4$ (vvw), $1147\cdot4$ (vw), $1324\cdot6$ (vvw), $2123\cdot6$ (vw), $2204\cdot9$ (vvw) and $2321\cdot5$ (vw). The first two, at least, must be overtones or combinations of low frequencies, of the rest 1147 appears quite strongly in the mixed crystal spectrum of McClure (1954), and is very probably a fundamental.

Comparison with solid-state spectra

The studies made by McClure (1954, 1956) to establish the assignment of this absorption system depended on the fact that mixed crystals of naphthalene in durene can be made in which the naphthalene molecules are isolated from one another, and are in known orientations relative to the axes of the host durene crystal. The result is that the absorption spectrum of naphthalene can be recorded under conditions closely approaching the ideal of the oriented gas; the polarization of individual transitions can be directly observed from the absorption of plane-polarized light incident on the mixed crystal. By this means McClure observed that the pure electronic band and bands separated from it by the frequencies of totally symmetrical vibrations were polarized parallel to the long molecular axis; a second set of bands, showing many of the same totally symmetrical intervals,

were polarized along the shorter axis. McClure identified two frequencies, 433 and 905 cm^{-1} , principally responsible for inducing the short-axis transitions, as non-totally symmetrical intervals, fundamentals or combinations, of symmetry b_{3g} . These conclusions broadly agree with those from the vapour spectrum, and a detailed comparison of the polarization of bands and frequency intervals shows an excellent agreement in detail. McClure gave a comparison of his measurements and the vapour frequencies and intensities of Henri & de Laszlo (1924) which showed a number of small discrepancies in frequency intervals and some serious differences in relative intensities. Many of the small frequency differences we find to be real, and are due to solid-state effects, including differences due to loss of rotational band structure, but the intensities were in many cases misjudged by Henri & de Laszlo, and there is in fact a fairly good agreement with the solid state intensity distribution. A number of bands observed by McClure are not found in the vapour. For example, there is no evidence in the vapour for the upper-state frequencies 747, 794 and 924 cm^{-1} which may owe their appearance in the solid state to crystal forces. Also a large number of the weaker vapour bands have not been observed in the mixed crystal. However, it is clear that the structure of the absorption system is the same in the two spectra and that McClure's claim that the mixed crystal spectrum is essentially that of the oriented gas is well justified.

The one important difficulty which was unresolved in the interpretation of the mixed crystal spectrum arose in the analysis of the fluorescence emission, which, like absorption, was recorded in its polarization dependence. McClure found that in fluorescence there were again two false origins as well as the true electronic origin for the vibrational progressions. One false origin was spaced by 509 cm^{-1} from the true origin and the other by 938 cm^{-1} . The first interval was identified with the strong polarized Raman frequency 512 cm^{-1} and thus assigned to the totally symmetrical species A_g . The second was also identified with a supposed totally symmetrical Raman frequency 943 cm^{-1} . These assignments cannot be reconciled with the fluorescence polarizations actually found, which show that the false origin bands are both short-axis polarized and the true origin long-axis polarized; the intervals concerned must therefore be non-totally symmetrical frequencies. As already indicated the vapour values of the perturbing frequencies are 506 and 936 cm^{-1} , the first being a new fundamental of b_{3g} symmetry and the second also of species b_{3g} ; the latter we think is the Raman-active 941 cm^{-1} hitherto incorrectly assigned or, less likely, it may be a new fundamental. With these frequencies and assignments the structure of the band system in mixed crystal fluorescence shows a substantial correspondence with the absorption spectrum. The ground state 506 cm^{-1} acts in the same way and with roughly the same perturbing power as the upper state 438 cm^{-1} , and 936 cm^{-1} acts like 911 cm^{-1} in the upper state. Also the recognition that 506 and 516 cm^{-1} are different vibrations removes the need for McClure's postulate that 438 cm^{-1} is a b_{3g} combination frequency. It seems clear that 506 and 438 cm^{-1} are fundamentals. We have already discussed the possible appearance of the 516 cm^{-1} vibration in fluorescence in combination with 506 cm^{-1} . A similar situation arises in the combination 0—938—516, which appears in McClure's mixed crystal fluorescence with the correct polarization for this assignment. In this case, the interval is fitted by the value 513 cm^{-1} . With this confirmation it seems established that both 506 and 516 cm^{-1} are active in mixed crystal

fluorescence, and that their polarizations are in harmony with assignments b_{3g} and a_g , respectively. There is thus a close analogy between the fluorescence and absorption spectra, and the same mechanism of vibrational perturbation affects each.

We now compare the vibration intervals measured in the mixed crystal and vapour spectra. The values are compared in table 4.

TABLE 4. VIBRATION FREQUENCIES IN MIXED CRYSTAL AND VAPOUR (CM^{-1})

vapour	mixed crystal	pentane solution (Bolotnikova 1959)	assignment
	(i) <i>ground state</i>		
506	509	495	b_{3g}
516* (?)	514 (?)	517	a_g
761	761	760	a_g
936	938	927	b_{3g}
	(ii) <i>excited state</i>		
438	433	—	b_{3g}
501	501	—	a_g
702	702	—	a_g
911	905	—	b_{3g}
987	987	—	a_g
1147	1145	—	a_g
1389	1386	—	a_g
1435	1429	—	a_g

* The vapour value is somewhat uncertain, being based only on the poorly resolved hot combination $0-1022$ seen as a double-headed band in the low-resolution plates. The assignment is taken to be $0-506-516$, since the only obvious alternative $0-1024$ has the wrong symmetry.

The comparison shows an interesting regularity. The values of totally symmetrical frequencies are very nearly the same in the two phases, while those of b_{3g} frequencies differ: in the ground state the vapour values are lower, and in the excited state higher, than the mixed crystal values. A part of the variation is a result of the different band contours of the vibrations in the vapour spectrum, as illustrated in figure 7. Measurements in the mixed crystal refer to band origins, and those in the vapour to band heads. In long-axis polarized absorption bands this maximum coincides nearly enough with the band origin; in short-axis polarized bands on the other hand the low-frequency maximum

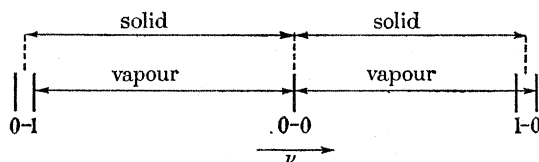


FIGURE 7. Relation between intervals measured in vapour and mixed crystal spectra. Full vertical lines refer to band heads or maxima, and dashed lines to band origins. The splitting of the vapour bands is exaggerated.

(which is the one recorded) lies between 1 and 2 cm^{-1} to low frequencies of the origin. Thus between bands of similar contour type the frequency intervals (totally symmetrical intervals) should be close to mixed crystal values; between bands of different contour type the intervals (non-totally symmetrical intervals) will differ systematically. If the double-headed band is higher in frequency than the single band the measured vapour interval is

bigger than the interval between the band origins, and vice versa. This difference should, however, not be greater than 1 or 2 cm^{-1} , but the differences recorded in table 8, while of the correct sign, are bigger than this, suggesting a further systematic cause acting in the same sense. The lower totally symmetrical intervals agree well in vapour and mixed-crystal spectra, while the higher ones tend to be *lower* in the crystal at least in the upper state.

Table 4 includes the values of ground-state frequencies recorded by Bolotnikova (1959) in the fluorescence spectrum in pentane at 77 °K. This spectrum shows clear evidence of two distinct frequencies near 500 cm^{-1} . Moreover, it shows a remarkable depression of both b_{3g} frequencies by about 10 cm^{-1} , while the two a_g frequencies of 517 and 760 cm^{-1} are unaffected by environment.

A number of calculations of the fundamental vibrations of naphthalene have been made, based on differing assumptions about force fields. The calculated values have had to be compared with experimental frequencies and assignments that are uncertain. The assignment of 506 cm^{-1} and 936 cm^{-1} as b_{3g} fundamentals eases this position somewhat. Scully & Whiffen (1958, private communication) noted the extreme sensitivity of the lowest b_{3g} frequency to the force field chosen: and thought that it may be hidden under the 512 cm^{-1} a_g frequency in the Raman spectrum. Schmid (1958) also got a near-coincidence of the lowest a_g and b_{3g} frequencies for one chosen force field. Subsequently, both Freeman & Ross (1961) and Scully & Whiffen (1961) have shown that these assignments, taken with other frequencies and assignments known from Raman measurements, are compatible with the results of calculation of normal vibrations from reasonable force fields. Some further information can be obtained when the naphthalene results are viewed with those for naphthalene *d*-8 which will be discussed in the following paper.

J. M. Hollas acknowledges the award of a British Celanese Studentship and S. C. Wait, Jr., the award of a Fulbright Scholarship. The authors also thank Messrs I.B.M. (United Kingdom) for generous arrangements made for the use of the I.B.M. 650 and 704 computers.

REFERENCES

- Abrahams, S. C., Robertson, J. M. & White, J. G. 1949 *Acta Cryst.* **2**, 238.
 Bolotnikova, T. N. 1959 *Izv. Akad. Nauk. SSSR, Ser. Fiz.* **23**, 28.
 Brandmuller, J. 1953 *Z. angew. Phys.* **5**, 95.
 Brandmuller, J. & Schmid, E. 1956 *Z. Phys.* **144**, 428.
 Braun, W. G., Spooner, D. F. & Fenske, M. R. 1950 *Anal. Chem.* **22**, 1074.
 Craig, D. P. 1950 *J. Chem. Soc.* p. 2146.
 Dennison, D. M. 1931 *Rev. Mod. Phys.* **3**, 280.
 Freeman, D. E. 1959 Thesis, University of Sydney.
 Freeman, D. E. & Ross, I. G. 1961 *Spectrochim. Acta*, **16**, 1393.
 Guilbert, J. 1955 Thesis, Paris.
 Henri, V. & de Laszlo, H. 1924 *Proc. Roy. Soc. A*, **105**, 668.
 Herzberg, G. 1945 *Infrared and Raman spectra*, p. 472. New York: van Nostrand.
 Joint Commission for Spectroscopy 1955 *J. Chem. Phys.* **23**, 1997.
 King, G. W. 1958 *J. Sci. Instrum.* **35**, 11.
 King, G. W., Hainer, R. M. & Cross, P. C. 1943 *J. Chem. Phys.* **11**, 27.
 King, G. W., Hainer, R. M. & Cross, P. C. 1956 *J. Chem. Phys.* **24**, 546.

- Knipe, R. H., Sponer, H. & Cooper, C. D. 1953 *J. Chem. Phys.* **21**, 376.
 Kohlrausch, K. I. V. F. 1943 *Handb. Jb. Chem. Phys.* Band 9/IV. Leipzig.
 Lippincott, E. R. & O'Reilly, E. J. 1955 *J. Chem. Phys.* **23**, 238.
 Luther, H. 1948 *Z. Elektrochem.* **52**, 210.
 Luther, H., Brandes, G., Gunzler, H. & Hampel, B. 1955 *Z. Elektrochem.* **59**, 1012.
 Luther, H., Feldman, K. & Hampel, B. 1955 *Z. Elektrochem.* **59**, 1008.
 Luther, H. & Hampel, B. 1950 *Z. Phys. Chem. A*, **202**, 390.
 McClure, D. S. 1954 *J. Chem. Phys.* **22**, 1668.
 McClure, D. S. 1956 *J. Chem. Phys.* **24**, 1.
 Mitra, S. S. & Bernstein, H. J. 1959 *Canad. J. Chem.* **37**, 355.
 Passerini, R. & Ross, I. G. 1954 *J. Chem. Phys.* **22**, 1012.
 Person, N. B., Pimentel, G. C. & Schnepp, O. 1955 *J. Chem. Phys.* **23**, 230.
 Prikhotjko, A. F. 1944 *J. Phys. U.S.S.R.* **8**, 257.
 Prikhotjko, A. F. 1949 *J. Exp. Theor. Phys. U.S.S.R.* **6**, 488.
 Schmid, E. 1958 *Z. Elektrochem.* **62**, 1005.
 Schnepp, O. & McClure, D. S. 1952 *J. Chem. Phys.* **20**, 1375.
 Scully, D. B. & Whiffen, D. H. 1961 *Spectrochim. Acta*, **16**, 1409.
 Sponer, H. & Nordheim, G. 1950 *Disc. Faraday Soc.* **9**, 19.
 Stein, M., Maschka, A., Wollrab, F. & Gnilsen, W. 1952 *Z. Phys. Chem.* **201**, 261.
 White, G. U. 1942 *J. Opt. Soc. Amer.* **32**, 285.

APPENDIX. FREQUENCIES (cm^{-1}) AND ASSIGNMENTS OF BAND HEADS
AND MAXIMA

The following is the complete list of measured maxima referred to as 'heads' hereafter. Assignments, where proposed, refer to the principal heads in table 2, and give the sequence intervals between the head concerned and the principal head. Thus

$$A_{0000}^{2300}$$

differs from the principal band head A by two sequence intervals in 10 cm^{-1} , and by three in 55 cm^{-1} . That is

$$32268.8 = 32457.9 - 2 \times 10 - 3 \times 56.4,$$

56.4 is the average sequence interval measured in this band group (individual values 56.6 , 56.3 , 56.3). The superscripts in order from the left refer to the sequence intervals 10 , 55 , 64 and 73 cm^{-1} , respectively, and the subscripts to 6 , 93 , 99 and 133 cm^{-1} , respectively. Roman letters refer to single-headed bands, and italics to double-headed bands. The higher frequency head of doubled bands is used for measurement; the lower head is recorded with ϵ added to the designation. Thus

$$A_{0000}^{2300} \quad \text{and} \quad A_{0000}^{2300} \epsilon$$

form a double-headed band, with heads at 32268.8 and 32266.2 cm^{-1} . The designation 'wing' refers to rotational structure associated with the named band, usually a very weak unresolved flat maximum to the red of the main maxima in doubled bands. Frequencies marked with an asterisk were measured from enlargements of the plates and are believed accurate $\pm 0.1 \text{ cm}^{-1}$. Others were measured directly, and are believed accurate to $\pm 0.05 \text{ cm}^{-1}$.

Doubtful assignments are shown in brackets.

NAPHTHALENE VAPOUR ABSORPTION BANDS AT 3200 Å. I 563

Frequencies and assignments of naphthalene h-8

(3200 Å system)

frequency	assnmt.	frequency	assnmt.	frequency	assnmt.	frequency	assnmt.
35 132.27	Ω_{0000}^{0000}	34 824.52*	$\Gamma_{1000}^{0000} \epsilon$	34 567.82*	Y_{0000}^{0100}	34 368.67*	—
30.25	$\Omega_{0000}^{0000} \epsilon$	21.40*	Γ_{0000}^{1000}	66.17*	Y_{0000}^{0000}	65.97	W_{0000}^{1100}
35 095.64	Ω_{0000}^{0000}	18.69*	$\Gamma_{0000}^{1000} \epsilon$	64.93*	$Y_{0000}^{0100} \epsilon$	64.99	V_{0000}^{0000}
86.93*	Δ_{0000}^{0000}	15.43*	—	63.77*	—	63.54	$W_{0000}^{1100} \epsilon, (W_{1000}^{2100})$
84.32*	$\Delta_{0000}^{0000} \epsilon$	12.50	—	60.45	(Z_{0000}^{1100})	62.30	$V_{0000}^{0000} \epsilon$
78.91	$(\Delta_{1000}^{0000} \epsilon)$	00.27	Δ_{0000}^{0100}	58.88	$(X_{0000}^{3000} \epsilon)$	54.81	—
76.91	Δ_{0000}^{1000}	34 796.06*	—	57.64	Z_{0000}^{2000}	54.17	V_{0000}^{1000}
74.33	$\Delta_{0000}^{1000} \epsilon$	90.75*	$(\Delta_{1000}^{0100} \epsilon)$	56.45	Y_{0000}^{1000}	52.21	$V_{0000}^{1000} \epsilon$
65.71*	Δ_{0000}^{2000}	88.13	Π_{0000}^{0100}	40.63*	—	51.63	—
63.29*	$\Delta_{0000}^{2000} \epsilon$	84.84	—	37.11*	X_{0000}^{0100}	44.55	V_{0000}^{2000}
59.79*	—	81.41*	—	35.79*	Γ_{0000}^{0100}	42.30	W_{0010}^{0000}
31.04	Δ_{0000}^{0100}	77.72*	Π_{0000}^{1100}	34.76*	(Δ_{0000}^{1200})	41.65	U_{0000}^{0000}
28.45	$\Delta_{0000}^{0100} \epsilon$	76.28*	Γ_{0000}^{0100}	15.42*	—	39.47	V_{0000}^{0100}
21.46*	Δ_{0000}^{1100}	72.67*	$\Gamma_{0000}^{0100} \epsilon$	13.42	$(X_{0000}^{2100} \epsilon)$	38.69	—
20.46*	Δ_{0000}^{0100}	71.02*	Γ_{1000}^{0100}	34 450.57	X_{0000}^{0000}	34.78*	(W_{0010}^{0000})
34 986.20	Δ_{0010}^{0000}	68.94*	$\Gamma_{1000}^{0100} \epsilon$	43.59*	X_{1000}^{0000}	22.26	$U_{0000}^{0000}, (V_{0010}^{0010})$
75.29	Δ_{0000}^{0200}	65.87*	Γ_{0000}^{1100}	42.28	—	19.79	$W_{0000}^{0200}, U_{0000}^{0000} \epsilon$
72.25*	$\Delta_{0000}^{0200} \epsilon$	63.61*	—	41.16	W_{0000}^{0000}	18.28	(W_{0000}^{1200})
64.81*	Δ_{0000}^{1200}	61.58*	—	37.16*	—	17.08*	$W_{0000}^{0200} \epsilon$
62.26	$\Delta_{0000}^{1200} \epsilon$	38.76	—	35.72*	W_{1000}^{0000}	08.99	V_{0000}^{0100}
40.99*	—	34.99*	—	33.08*	—	08.17	W_{0001}^{0000}
40.19*	—	34 655.52	Δ_{0000}^{0000}	32.40	W_{0000}^{0000}	06.41	$V_{0000}^{0100} \epsilon$
05.00	Π_{0000}^{0000}	53.37	—	30.96	W_{0000}^{1000}	04.49	—
02.33*	$\Pi_{0000}^{0000} \epsilon$	46.15*	—	29.79	$W_{0000}^{0000} \epsilon$	01.92	—
34 894.71*	Π_{0000}^{1000}	45.34*	Δ_{0000}^{1000}	25.24	W_{1000}^{1000}	34 299.02	V_{0000}^{1100}
92.19*	$\Pi_{0000}^{1000} \epsilon$	43.54*	—	23.34	—	97.75	—
88.73*	—	42.65*	—	22.38	W_{0000}^{1000}	96.38	$V_{0000}^{1100} \epsilon$
87.75*	—	35.68	—	20.67	W_{0000}^{2000}	94.69	—
85.70	Δ_{0000}^{0000}	25.01	Z_{0000}^{0000}	19.82	$W_{0000}^{1000} \epsilon$	93.80	—
82.57	—	23.70	Y_{0000}^{0000}	16.92*	—	92.13	—
79.05	—	22.47	$Z_{0000}^{0000} \epsilon$	14.24*	W_{1000}^{2000}	89.32*	—
75.61	Δ_{0000}^{1000}	21.16	$Y_{1000}^{0000} \epsilon$	12.52*	W_{0000}^{2000}	86.05*	U_{0000}^{0100}
74.07	—	18.24	Y_{1000}^{0000}	10.64*	W_{0000}^{3000}	82.04*	—
71.33*	—	15.48*	Z_{0000}^{1000}	09.93*	$W_{0000}^{2000} \epsilon$	79.02*	—
68.48*	—	04.06*	—	09.22*	—	76.09*	U_{0000}^{1100}
67.87*	—	00.64*	Δ_{0000}^{0100}	09.38*	—	73.02*	—
65.05*	Δ_{0000}^{2000}	34 597.66*	—	34 396.12	V_{0000}^{0000}	58.74	—
63.16*	—	93.81	—	91.95*	—	37.59	$T_{0000}^{0000} \epsilon$
57.62	—	92.00	X_{0000}^{0000}	89.98*	V_{1000}^{0000}	34.94*	T_{0000}^{0000}
56.17	Δ_{0000}^{0000}	91.60*	Γ_{0000}^{0000}	87.53	—	34.12*	—
53.52	$\Delta_{0000}^{0000} \epsilon$	90.84*	Δ_{0000}^{1100}	86.01	V_{0000}^{1000}	25.13	T_{0000}^{0000}
49.25	Δ_{1000}^{0000}	89.35	$X_{0000}^{0000} \epsilon$	85.15	W_{0000}^{0100}	22.61*	—
46.40	$\Delta_{1000}^{0000} \epsilon$	81.99*	X_{1000}^{0000}	84.31	—	18.98	T_{1000}^{0000}
41.97	Π_{0000}^{0000}	80.01*	—	78.94	W_{1000}^{0100}	17.64*	—
35.38*	Π_{1000}^{0000}	79.08	$X_{0000}^{1000} \epsilon$	76.95	—	14.27*	T_{0000}^{1000}
31.80	Γ_{0000}^{0000}	78.28	Z_{0000}^{0000}	75.56	W_{0000}^{0100}	11.92*	—
28.92*	$\Gamma_{0000}^{0000} \epsilon$	71.75	X_{0000}^{2000}	74.39	(W_{0000}^{1100})	09.20*	—
26.76*	Γ_{1000}^{0000}	68.93*	$X_{0000}^{2000} \epsilon$	73.11	$W_{0000}^{0100} \epsilon$		

Frequencies and assignments

frequency	assnmt.	frequency	assnmt.	frequency	assnmt.	frequency	assnmt.
34 206.76*	U ₀₀₀₁ ⁰⁰⁰⁰	34 029.68*	—	33 901.45	—	33 817.55	—
03.91*	T ₀₀₀₀ ²⁰⁰⁰	26.44*	—	00.27*	(P ₁₀₀₀ ¹⁰⁰⁰ ε)	15.76	—
01.35*	—	23.60*	—			14.19	—
34 196.50	—	15.53*	—	33 899.36	—	13.48	N ₀₀₀₀ ⁰¹⁰⁰
94.08*	T ₀₀₀₀ ³⁰⁰⁰	12.11*	R ₀₀₀₁ ⁰⁰⁰⁰	98.15	Q ₀₀₀₀ ⁰¹⁰⁰ , P ₀₀₀₀ ²⁰⁰⁰	11.64	—
83.94*	—	08.19*	—	95.57	P ₀₀₀₀ ²⁰⁰⁰ ε	10.72	N ₀₀₀₀ ⁰¹⁰⁰ ε
76.51	S ₀₀₀₀ ⁰⁰⁰⁰	05.31*	—	94.95	—	07.45	P ₀₀₀₀ ⁰²⁰⁰
73.99	S ₀₀₀₀ ⁰⁰⁰⁰ ε	02.79*	—	94.09*	—	06.72	N ₁₀₀₀ ⁰¹⁰⁰
65.65	S ₀₀₀₀ ¹⁰⁰⁰			92.23	O ₀₀₀₀ ⁰⁰⁰⁰	03.57	N ₀₀₀₀ ¹¹⁰⁰
56.62	—	33 998.09*	—	91.21	O ₀₀₀₀ ⁰⁰⁰⁰ (wing)	00.75	N ₀₀₀₀ ¹¹⁰⁰ ε
55.67	—	95.41	—	89.47	O ₀₀₀₀ ⁰⁰⁰⁰ ε	33 794.79	N ₀₀₀₀ ⁰⁰⁰¹
46.00	R ₀₀₀₀ ⁰⁰⁰⁰	94.68	R ₀₀₀₀ ⁰⁰⁰⁰	88.41	O ₀₀₀₀ ⁰⁰⁰⁰ ε (wing)	93.10	N ₀₀₀₀ ²¹⁰⁰ , O ₀₀₁₀ ⁰⁰⁰⁰
43.82	S ₀₀₀₀ ⁰⁰⁰⁰	92.59	—	87.28	—	78.01*	O ₀₀₀₀ ⁰²⁰⁰
43.23	R ₀₀₀₀ ⁰⁰⁰⁰ ε	91.37*	—	85.44	O ₁₀₀₀ ⁰⁰⁰⁰	77.24	N ₀₁₀₀ ⁰⁰⁰⁰
42.26	—	89.73*	—	82.82	O ₁₀₀₀ ⁰⁰⁰⁰ ε	63.34*	—
39.80*	R ₁₀₀₀ ⁰⁰⁰⁰	87.66	—	82.01	O ₁₀₀₀ ⁰⁰⁰⁰	61.34	—
39.08*	S ₁₀₀₀ ⁰⁰⁰⁰	87.03*	—	81.18	O ₁₀₀₀ ⁰⁰⁰⁰ (wing)	58.64*	O ₀₀₀₁ ⁰⁰⁰⁰
35.98	R ₁₀₀₀ ⁰⁰⁰⁰	84.68	R ₁₀₀₀ ⁰⁰⁰⁰	79.28	O ₁₀₀₀ ⁰⁰⁰⁰ ε	57.51*	—
33.86	S ₁₀₀₀ ⁰⁰⁰⁰	81.42	—	78.06*	O ₁₀₀₀ ⁰⁰⁰⁰ ε (wing)	35.60	O ₀₀₀₀ ⁰⁰⁰⁰ , (N ₀₀₀₁ ⁰⁰⁰⁰)
33.23	R ₁₀₀₀ ⁰⁰⁰⁰ ε	78.67*	—	75.24*	O ₁₀₀₀ ⁰⁰⁰⁰	30.10*	O ₁₀₀₀ ⁰⁰⁰⁰
23.95	S ₂₀₀₀ ⁰⁰⁰⁰	76.70	Q ₀₀₀₀ ⁰⁰⁰⁰	72.86	O ₁₀₀₀ ⁰⁰⁰⁰ ε	25.01	O ₁₀₀₀ ⁰⁰⁰⁰
21.42	—	74.05	Q ₀₀₀₀ ⁰⁰⁰⁰ ε	71.98	O ₂₀₀₀ ⁰⁰⁰⁰	22.60	—
20.58	—	70.58*	Q ₁₀₀₀ ⁰⁰⁰⁰	69.15	N ₀₀₀₀ ⁰⁰⁰⁰ , O ₀₀₀₀ ²⁰⁰⁰ ε	20.52	—
17.98*	—	68.04*	Q ₁₀₀₀ ⁰⁰⁰⁰ ε	66.52	N ₀₀₀₀ ⁰⁰⁰⁰ ε	12.99	—
15.77*	—	66.62	Q ₁₀₀₀ ⁰⁰⁰⁰	65.41	N ₀₀₀₀ ⁰⁰⁰⁰ ε (wing)	10.65*	—
13.92*	S ₃₀₀₀ ⁰⁰⁰⁰	63.89	Q ₁₀₀₀ ⁰⁰⁰⁰ ε	64.32	—	04.13	—
11.24	—	60.35*	Q ₁₀₀₀ ⁰⁰⁰⁰	62.72	N ₁₀₀₀ ⁰⁰⁰⁰ , P ₀₀₀₀ ⁰¹⁰⁰	02.50	—
08.90*	—	58.81*	—	60.08	N ₁₀₀₀ ⁰⁰⁰⁰ ε, P ₀₀₀₀ ⁰¹⁰⁰ ε	01.52	—
08.23*	—	55.95	—	59.18	N ₁₀₀₀ ⁰⁰⁰⁰	33 696.87	—
04.71*	—	54.83	Q ₀₀₀₀ ⁰⁰⁰⁰	56.50	N ₁₀₀₀ ⁰⁰⁰⁰ ε	94.31*	—
03.91*	S ₀₀₀₀ ⁰⁰⁰⁰	52.34*	—	53.47*	P ₀₀₁₀ ⁰⁰⁰⁰	83.66	—
03.27*	—	50.93	—	52.65	P ₁₁₀₀ ⁰⁰⁰⁰	79.77*	O ₀₁₀₀ ⁰⁰⁰⁰
02.22*	—	49.19	Q ₁₀₀₀ ⁰⁰⁰⁰	51.57	—	73.45	—
34 096.82*	—	46.06	—	50.80	—	69.10	O ₁₁₀₀ ⁰⁰⁰⁰
91.64	R ₀₁₀₀ ⁰⁰⁰⁰	45.77	Q ₁₀₀₀ ⁰⁰⁰⁰	50.04	P ₁₁₀₀ ⁰⁰⁰⁰ ε	67.70*	—
90.34	—	43.00	P ₀₀₀₀ ⁰⁰⁰⁰	49.22	N ₂₀₀₀ ⁰⁰⁰⁰	58.83	M ₀₀₀₀ ⁰⁰⁰⁰
89.23	R ₀₁₀₀ ⁰⁰⁰⁰ ε	40.93*	—	46.50	N ₂₀₀₀ ⁰⁰⁰⁰ ε	56.14	M ₀₀₀₀ ⁰⁰⁰⁰ ε
85.32	—	38.87*	P ₀₀₀₀ ¹⁰⁰⁰	45.52*	P ₀₀₀₁ ⁰⁰⁰⁰	49.35	M ₁₀₀₀ ⁰⁰⁰⁰
81.75	R ₁₁₀₀ ⁰⁰⁰⁰	36.86	Q ₀₀₀₀ ²⁰⁰⁰	45.00*	—	46.03*	—
81.16*	R ₀₀₁₀ ⁰⁰⁰⁰	34.38*	—	42.63*	P ₂₁₀₀ ⁰⁰⁰⁰	40.97	—
79.20	R ₁₁₀₀ ⁰⁰⁰⁰ ε	33.23	P ₁₀₀₀ ⁰⁰⁰⁰	41.67	Q ₀₀₀₀ ⁰²⁰⁰	40.35	L ₀₀₀₀ ⁰⁰⁰⁰
78.38	R ₀₀₁₀ ⁰⁰⁰⁰ ε	24.34	—	39.95	P ₂₁₀₀ ¹⁰⁰⁰ ε	38.25	K ₀₀₀₀ ⁰⁰⁰⁰
72.13	R ₂₁₀₀ ⁰⁰⁰⁰	21.73	—	39.21	N ₃₀₀₀ ⁰⁰⁰⁰	37.46	L ₀₀₀₀ ⁰⁰⁰⁰ ε
71.36	R ₁₀₁₀ ⁰⁰⁰⁰	19.75	—	35.00	O ₀₁₀₀ ⁰⁰⁰⁰	36.36	L ₀₀₀₀ ⁰⁰⁰⁰ ε (wing)
69.52*	R ₂₁₀₀ ⁰⁰⁰⁰ ε	19.15	—	33.67	O ₀₁₀₀ ⁰⁰⁰⁰ (wing)	35.40	K ₀₀₀₀ ⁰⁰⁰⁰
50.05*	—	18.20	P ₀₀₀₀ ⁰⁰⁰⁰	32.39	O ₀₁₀₀ ⁰⁰⁰⁰ ε	34.59	K ₀₀₀₀ ⁰⁰⁰⁰ ε (wing)
47.69*	R ₀₀₁₀ ⁰⁰⁰⁰	15.56	P ₀₀₀₀ ⁰⁰⁰⁰ ε	31.39	—	33.71	L ₁₀₀₀ ⁰⁰⁰⁰
45.37*	R ₀₀₁₀ ⁰⁰⁰⁰ ε	14.43	—	30.80	—	33.25	—
43.00	—	13.44	P ₀₀₀₀ ¹⁰⁰⁰	29.77	—	32.13	K ₀₀₀₀ ¹⁰⁰⁰
40.33	—	12.62	—	25.79*	O ₀₀₁₀ ⁰⁰⁰⁰ , (P ₀₁₀₀ ⁰⁰⁰⁰)	30.61	L ₁₀₀₀ ⁰⁰⁰⁰
39.46	—	10.72	P ₀₀₀₀ ¹⁰⁰⁰ ε	24.89*	O ₁₁₀₀ ⁰⁰⁰⁰	29.47	K ₀₀₀₀ ¹⁰⁰⁰ ε
36.37*	—	10.00	—	22.09*	O ₁₁₀₀ ⁰⁰⁰⁰ ε	28.26	K ₁₀₀₀ ⁰⁰⁰⁰
30.92*	—	08.11	P ₁₀₀₀ ⁰⁰⁰⁰	19.37	P ₀₀₀₀ ⁰⁰¹⁰	27.62	L ₁₀₀₀ ⁰⁰⁰⁰ ε
		05.50	P ₁₀₀₀ ⁰⁰⁰⁰ ε	18.78	O ₀₀₀₁ ⁰⁰⁰⁰		

NAPHTHALENE VAPOUR ABSORPTION BANDS AT 3200 Å. I 565

frequency	assnmt.	frequency	assnmt.	frequency	assnmt.	frequency	assnmt.
33 626.90	J_{0000}^{0000}	33 519.76	—	33 389.53	K_{0000}^{2000}	33 301.61	—
25.54	$K_{0000}^{1000} \epsilon$	18.81	L_{0000}^{1200}	88.92	I_{0000}^{0100}	00.75	—
24.32	$J_{0000}^{0000} \epsilon$	17.26*	—	88.53	L_{0000}^{1100}	33 295.27*	—
20.98	L_{0000}^{2000}	16.00	$L_{0000}^{1200} \epsilon$	86.25	$I_{0000}^{0100} \epsilon$	94.10	—
18.48	K_{0000}^{2000}	13.28	—	83.29	I_{1000}^{0100}	92.69	—
17.86	$L_{0000}^{2000} \epsilon$	09.27*	—	81.76	J_{0000}^{2000}	91.49	—
17.12	J_{0000}^{1000}	07.98	N_{0000}^{0000}	80.69	$I_{1000}^{0100} \epsilon$	89.94	I_{0010}^{1000}
15.82	$K_{0000}^{2000} \epsilon$	07.09	—	80.21	I_{0000}^{0010}	88.27	I_{0000}^{1000}
14.49	$J_{0000}^{1000} \epsilon$	03.33	N_{1000}^{0000}	78.90	I_{0000}^{1100}	87.17	L_{0000}^{0300}
13.12	—	33 499.14	N_{0000}^{1000}	78.27	L_{0000}^{2100}	84.62	—
08.14	(K_{0000}^{3000})	95.96*	M_{0000}^{0000}	77.53	$I_{0000}^{0010} \epsilon$	83.59	—
07.25	J_{0000}^{2000}	90.20*	N_{0000}^{2000}	76.22	$I_{0000}^{1100} \epsilon$	79.09	—
06.38	—	87.75*	—	73.01	I_{0000}^{0001}	78.12	I_{0000}^{1100}
04.14	$M_{0000}^{0100}, J_{0000}^{2000} \epsilon$	74.18*	L_{0000}^{0300}	71.32	J_{0000}^{3000}	76.97*	$L_{0000}^{1300}, I_{0000}^{0300}$
01.43	$M_{0000}^{0100} \epsilon$	71.48	$L_{0000}^{0300} \epsilon$	70.20	$I_{0000}^{0001} \epsilon$	74.70	$I_{0000}^{0300} \epsilon$
00.50*	$M_{0000}^{0100} \epsilon$ (wing)	60.05*	—	68.96	I_{0000}^{2100}	67.14*	I_{0000}^{1300}
33 597.21*	J_{0000}^{3000}	57.87*	—	67.96	H_{0000}^{0000}	66.73	L_{0000}^{2300}
95.31*	—	55.76	—	65.73	$(H_{0000}^{0000} \epsilon)$	64.59	$I_{0000}^{1300} \epsilon$
94.08*	M_{0000}^{1100}	54.91	L_{0000}^{0000}	64.96	—	63.04*	—
92.87*	—	52.84	—	61.17	L_{0000}^{0010}	57.70	—
91.22	$M_{0000}^{1100} \epsilon$	51.75	N_{0000}^{0100}	59.43*	—	56.50*	L_{0000}^{3300}
87.81	—	48.97	L_{1000}^{0000}	57.86	H_{1000}^{0000}	53.18*	—
84.52	L_{0000}^{0100}	47.74	N_{1000}^{0100}	56.05	L_{0010}^{0000}	51.00	—
81.93	K_{0000}^{0100}	45.44	I_{0000}^{0000}	54.68*	K_{0000}^{0100}	44.11	—
81.44	$L_{0000}^{0100} \epsilon$	44.69	L_{0000}^{1000}	52.79	—	22.48*	—
79.01*	$K_{0000}^{0100} \epsilon$	42.76	$I_{0000}^{0000} \epsilon$	51.97	—	21.52*	I_{0000}^{0000}
77.48*	L_{1000}^{0100}	40.23	I_{1000}^{0000}	51.08	—	20.55	G_{0000}^{0000}
76.54*	K_{1000}^{0100}	38.40	L_{1000}^{1000}	49.82	—	17.71	$G_{0000}^{0000} \epsilon$
74.55	$L_{0000}^{1100}, I_{0000}^{0010}$	37.63	$I_{1000}^{0000} \epsilon$	48.84	I_{0000}^{0100}	16.78	—
72.03	K_{1000}^{1100}	35.38	I_{1000}^{0000}	47.53*	H_{2000}^{0000}	14.29	G_{1000}^{0000}
71.77*	$L_{1000}^{1100} \epsilon$	34.48	L_{2000}^{0000}	46.08	I_{0010}^{0000}	12.20	H_{0000}^{0000}
69.17	$K_{1000}^{1100} \epsilon$	32.76	$I_{1000}^{0000} \epsilon$	44.83	I_{0000}^{0000}	10.45	G_{1000}^{0000}
66.67*	—	29.56	I_{1000}^{0000}	43.35	$I_{0010}^{0000} \epsilon$	07.59	$G_{0000}^{1000} \epsilon$
64.84*	L_{2000}^{1000}	27.05	$I_{1000}^{0000} \epsilon$	42.81	L_{0000}^{0200}	01.73	H_{1000}^{0000}
62.53*	J_{0000}^{0010}	25.37	I_{2000}^{0000}	38.57	L_{1000}^{0200}	00.29	G_{0000}^{2000}
61.61*	$L_{0000}^{2100} \epsilon$	24.22	L_{0000}^{3000}	36.29*	I_{0010}^{1000}	33 197.30	$G_{0000}^{2000} \epsilon$
59.25	—	22.74	$I_{0000}^{0000} \epsilon$	34.82	I_{0000}^{1000}	91.20	H_{2000}^{0000}
58.47	—	19.92	I_{1000}^{2000}	33.76*	$I_{0010}^{1000} \epsilon$	89.82	F_{0000}^{0000}
57.55	—	17.36	$I_{1000}^{2000} \epsilon$	32.89	I_{0000}^{0200}	87.13	$F_{0000}^{0000} \epsilon$
56.63*	—	16.77	—	32.56	L_{0000}^{1200}	84.36	F_{0000}^{0000}
54.95	L_{0000}^{3100}	15.44*	I_{0000}^{3000}	30.23	$I_{0000}^{0200} \epsilon$	81.72	$F_{0000}^{0000} \epsilon$
51.73*	$L_{0000}^{3100} \epsilon$	14.04	L_{0000}^{4000}	23.99	—	79.89	$F_{0000}^{1000} \epsilon$
47.40	L_{0000}^{0010}	12.73	$I_{0000}^{3000} \epsilon$	22.69	I_{0000}^{1200}	77.16	$F_{1000}^{0000} \epsilon$
44.68	$L_{0000}^{0010} \epsilon$	10.56	—	22.25	L_{0000}^{2200}	71.33	—
43.95	K_{0000}^{0100}	09.71	K_{0000}^{0000}	21.30	L_{0001}^{0000}	69.92	F_{2000}^{0000}
40.96	$K_{0000}^{0100} \epsilon$	07.83*	—	20.03	$I_{0000}^{1200} \epsilon$	67.60	G_{0000}^{0000}
38.08	—	06.77*	—	18.88	—	65.70*	G_{0000}^{0100}
37.34	L_{0000}^{1000}	05.32	I_{0000}^{4000}	17.05*	K_{0000}^{0100}	62.43	G_{1000}^{0000}
36.17	(J_{0000}^{0010})	03.18	J_{0000}^{0000}	15.14	—	59.62	—
32.62	—	00.55	—	11.67*	—	58.50	E_{0000}^{0000}
32.35	—	33 399.62	K_{0000}^{1000}	09.18	K_{0000}^{0010}	57.46	E_{0000}^{0000} (wing)
29.14	L_{0000}^{0200}	98.69	L_{0000}^{0100}	07.00	—	55.77	$E_{0000}^{0000} \epsilon$
26.47	$L_{0000}^{0200} \epsilon$	93.23	L_{1000}^{0100}	06.10	—	54.70	$E_{0000}^{0000} \epsilon$ (wing)
23.58*	—	92.20	J_{0000}^{1000}	02.38	—	52.02	E_{1000}^{0000}

Frequencies and assignments

frequency	assnmt.	frequency	assnmt.	frequency	assnmt.	frequency	assnmt.
33 151.40	E_{1000}^{0000} (wing)	33 059.40	E_{0010}^{0000}	32 918.46	$B_{0000}^{1000} \epsilon$	32 810.85	B_{0000}^{1200}
49.29	$E_{1000}^{0000} \epsilon$	56.31	$E_{0010}^{0000} \epsilon, F_{0000}^{0200}$	15.53	$B_{1000}^{1000} \epsilon$	08.10	B_{0000}^{1200}
48.49	E_{0000}^{1000}	53.36	—	12.85	$B_{1000}^{1000} \epsilon$	00.75	B_{0000}^{2200}
46.22	$E_{0000}^{1000} \epsilon$ (wing?)	52.72	—	11.22	B_{0000}^{2000}	32 799.86	B_{0001}^{0000}
45.66	$E_{0000}^{1000} \epsilon$	51.34	—	08.52	$B_{0000}^{2000} \epsilon$	98.03	$B_{0000}^{2000} \epsilon$
42.74*	—	50.15	—	05.15	B_{1000}^{2000}	97.67	$(B_{0001}^{0000} \epsilon)$
41.69	E_{1000}^{1000}	48.44	E_{0000}^{0200}	02.64*	$B_{1000}^{2000} \epsilon$	94.28	—
41.09	$E_{1000}^{1000} \epsilon$ (wing)	46.47	—	01.27	B_{0000}^{3000}	87.96	B_{1000}^{0100}
39.03	$E_{1000}^{1000} \epsilon$	45.46	$E_{0000}^{0200} \epsilon$	32 898.49	$B_{0000}^{3000} \epsilon$	85.01	$B_{1000}^{0100} \epsilon$
38.47	E_{0000}^{2000}	41.55	E_{1000}^{0200}	96.46	F_{0000}^{0200}	81.82*	—
36.54*	E_{0000}^{2000} (wing)	38.65	E_{0000}^{1200}	92.43*	$(B_{1000}^{3000} \epsilon)$	79.06*	—
35.69	$E_{0000}^{2000} \epsilon$	35.70	$E_{0000}^{1200} \epsilon$	91.24	B_{0000}^{4000}	77.68*	—
33.79	F_{0000}^{0100}	34.41*	$(E_{0000}^{0110} \epsilon)$	88.52	$B_{0000}^{4000} \epsilon$	76.72	—
31.29	$F_{0000}^{0100} \epsilon$	30.30	—	87.59	—	75.78	—
28.41	E_{0000}^{3000}	28.93	E_{0000}^{2200}	76.41	—	74.83	B_{0000}^{0100}
27.22	D_{0000}^{0000}	23.63	—	75.91	B_{0000}^{0100}	72.03	$B_{0010}^{0100} \epsilon$
25.67	$E_{0000}^{3000} \epsilon$	21.53	—	73.14	$B_{0000}^{0100} \epsilon$	68.96	—
24.55	$D_{0000}^{0000} \epsilon$	18.91*	E_{0000}^{3200}	70.00	B_{1000}^{0100}	65.96	B_{0000}^{0300}
21.15*	D_{1000}^{0000}	15.95*	—	67.34	$B_{1000}^{0100} \epsilon$	63.24	$B_{0000}^{0300} \epsilon$
17.06	D_{1000}^{0000}	13.29*	—	66.31	B_{0000}^{0010}	62.20	—
14.41	$D_{1000}^{0000} \epsilon$	07.64	F_{0000}^{0000}	65.87	B_{1000}^{0000}	59.46	B_{0000}^{0300}
11.72	G_{0000}^{0100}	02.91	F_{1000}^{0000}	63.59	$B_{0000}^{0010} \epsilon$	55.94	B_{0000}^{1300}
08.92	—	32 997.64	F_{0000}^{1000}	63.09	$B_{0000}^{1100} \epsilon$	53.16	$B_{0000}^{1300} \epsilon$
08.17	—	95.54	—	60.34	—	45.82	B_{0000}^{2300}
05.01	G_{1000}^{0100}	92.74	E_{0000}^{0300}	59.79	B_{1000}^{1000}	43.11	$B_{0000}^{2300} \epsilon$
04.19	E_{0000}^{0100}	91.78	F_{1000}^{1000}	57.64	B_{0000}^{0000}	28.41*	B_{0020}^{0000}
02.27	—	87.56	F_{0000}^{2000}	57.08	$B_{1000}^{1000} \epsilon$	23.82	—
01.37	$E_{0000}^{0100} \epsilon$	80.62*	F_{1000}^{2000}	56.34	B_{0000}^{1010}	22.15	E_{0000}^{0000}
33 097.29	E_{1000}^{0100}	76.22	—	55.83	B_{0000}^{2100}	19.95*	B_{0010}^{0200}
94.36	E_{1000}^{0100}	71.51*	—	53.68	$B_{0000}^{1010} \epsilon$	17.42	$B_{0010}^{0200} \epsilon$
93.44	E_{0000}^{0010}	67.85*	—	53.16	$B_{0000}^{2100} \epsilon$	15.54	E_{1000}^{0000}
91.44	$E_{0000}^{1100} \epsilon$	65.06*	—	47.52	B_{0000}^{1001}	12.31	E_{0000}^{1000}
90.64	$E_{0000}^{0010} \epsilon$	58.23	C_{0000}^{0000}	45.82	B_{0000}^{3100}	08.67	—
87.16*	E_{1000}^{1100}	55.42	$C_{0000}^{0000} \epsilon$	45.23	—	06.89	—
85.94	—	52.80	C_{0000}^{0000}	43.69	—	04.24	—
84.94	E_{0000}^{0000}	51.94	F_{0000}^{0100}	43.14	$B_{0000}^{3100} \epsilon$	02.48	E_{0000}^{2000}
84.43	E_{0000}^{2100}	51.33	—	42.21	—	32 693.92	—
83.49	E_{0000}^{1010}	49.52*	$C_{0000}^{1000} \epsilon$	40.90	$B_{0000}^{0000} \epsilon$	92.63	E_{0000}^{3000}
82.89	—	48.62	—	39.56	—	82.73	E_{0000}^{4000}
81.55	$E_{0000}^{2100} \epsilon$	46.71	F_{0000}^{0100}	37.05	—	71.65	—
80.88	$E_{0000}^{1010} \epsilon$	43.04	F_{0000}^{0010}	35.04	—	67.73	E_{0000}^{0100}
79.22*	—	41.94	F_{0000}^{1100}	34.26	—	57.81	E_{0000}^{1100}
78.31*	—	40.13*	—	33.28*	(B_{1000}^{1000})	56.32	E_{0010}^{0000}
76.81*	—	37.60*	—	31.71	—	54.26	—
75.75	—	34.98	—	30.74	$B_{0000}^{1000} \epsilon$	50.75	—
74.62	E_{0000}^{3100}	32.65*	—	29.65	B_{0010}^{0000}	48.17	E_{0000}^{2100}
73.93	—	31.15	B_{0000}^{0000}	26.83	$B_{0010}^{0000} \epsilon$	40.64*	—
71.66	$E_{0000}^{3100} \epsilon$	28.40	$B_{0000}^{0000} \epsilon$	24.48	B_{0010}^{0000}	37.99*	E_{0000}^{3100}
71.13*	—	27.42	$B_{0000}^{0000} \epsilon$ (wing)	20.82	B_{0000}^{0200}	29.72	E_{0000}^{0100}
69.75*	—	25.74	B_{0000}^{1000}	19.93	B_{0010}^{1000}	23.42*	—
68.92	—	24.82	B_{0000}^{1000}	18.09	$B_{0000}^{0200} \epsilon$	19.44	E_{0000}^{1000}
66.31*	E_{0000}^{0100}	22.99	$B_{0000}^{1000} \epsilon$	17.16	$B_{0000}^{1000} \epsilon$	18.33	E_{0000}^{0010}
62.96*	—	21.21	B_{0000}^{1000}	14.48	B_{0000}^{0200}	15.61*	E_{0000}^{0200}
60.50	—	19.73	$B_{0000}^{1000} \epsilon$ (wing)	11.88	B_{0000}^{0200}	12.63	—

NAPHTHALENE VAPOUR ABSORPTION BANDS AT 3200 Å. I 567

frequency	assnmt.	frequency	assnmt.	frequency	assnmt.	frequency	assnmt.
32 610.79	—	32 446.21	—	32 351.02	$A_{1010}^{0000} \epsilon$	32 263.86	—
08.57	E_{0010}^{1000}	45.27	$A_{0000}^{1000} \epsilon$	49.42	A_{0010}^{1000}	59.83*	—
06.14*	E_{0000}^{1200}	41.81	A_{1000}^{1000}	46.57	$A_{0010}^{1000} \epsilon$	48.12*	—
02.61*	—	39.20	$A_{1000}^{1000} \epsilon$	45.82	—	47.27*	A_{0010}^{0200}
00.30*	—	38.05	A_{0000}^{2000}	45.11	A_{0000}^{0200}	44.15*	$A_{0010}^{0200} \epsilon$
32 599.09*	E_{0010}^{2000}	35.29	$A_{0000}^{2000} \epsilon$	42.30	$A_{0000}^{0200} \epsilon$	43.56*	—
94.93	—	32.58	—	39.68	A_{0010}^{2000}	37.93*	—
92.41	E_{0001}^{0000}	31.16	A_{1000}^{2000}	38.65	A_{1000}^{0200}	34.62*	—
89.19	—	30.05	—	36.88*	$A_{0010}^{2000} \epsilon$	33.02	A_{0000}^{0400}
82.04	—	28.73	$A_{1000}^{2000} \epsilon$	35.90	A_{0000}^{0110}	30.28	$A_{0000}^{0400} \epsilon$
76.31	E_{0100}^{0100}	28.09	A_{0000}^{3000}	35.08	A_{1200}^{0000}	28.75*	—
65.13*	E_{0010}^{0100}	25.32	$A_{0000}^{3000} \epsilon$	33.10	$A_{0110}^{0000} \epsilon$	26.94*	Φ_{0000}^{0000}
61.61	D_{0000}^{0000}	21.93*	A_{1000}^{3000}	32.29	$A_{1200}^{0000} \epsilon$	24.16*	$\Phi_{0000}^{0000} \epsilon$
55.26*	D_{1000}^{0000}	19.31*	$A_{1000}^{3000} \epsilon$	30.51	A_{0101}^{0000}	18.98*	—
51.15	D_{0000}^{1000}	18.08	A_{0000}^{4000}	28.28	$A_{0101}^{0000} \epsilon$	16.01*	—
45.56	D_{1000}^{1000}	15.31	$A_{0000}^{4000} \epsilon$	27.76	A_{0001}^{0000}	32 174.63*	$(A_{0000}^{0500} \epsilon)$
40.76	D_{0000}^{2000}	11.58*	A_{1000}^{4000}	25.98	A_{1110}^{0000}	70.98*	Φ_{0000}^{0100}
39.53	—	09.18	C_{0000}^{0200}	25.02	$A_{0000}^{2200}, A_{0001}^{0000} \epsilon$	68.19*	$\Phi_{0000}^{0100} \epsilon$
36.90	—	08.10*	A_{0000}^{5000}	23.11	$A_{1110}^{0000} \epsilon$	61.30	—
34.87	D_{1000}^{2000}	05.23*	$A_{0000}^{5000} \epsilon$	22.29	$A_{2200}^{0000} \epsilon$	60.80	Φ_{0000}^{1100}
32.62*	—	02.06	—	20.23	—	60.28	—
30.10	D_{0000}^{3000}	01.38	A_{0000}^{0100}	19.36*	—	48.25*	—
20.93	C_{0000}^{0000}	32 399.24	—	17.59	A_{0001}^{1000}	39.66	—
15.70	C_{1000}^{0000}	98.62	$A_{0000}^{0100} \epsilon$	15.97	A_{2110}^{0000}	37.27	—
12.29	C_{0000}^{1000}	95.33	A_{1000}^{0100}	14.88*	A_{3200}^{0000}	14.89	Φ_{0000}^{0200}
10.02	—	92.40	A_{0000}^{0010}	12.24	$A_{3200}^{0000} \epsilon$	12.18	$\Phi_{0000}^{0200} \epsilon$
08.91	B_{0000}^{0000}	91.39	A_{1100}^{0000}	09.13*	—	32 059.34	Φ_{0000}^{0300}
06.65	D_{0000}^{0100}	89.58	$A_{0000}^{0010} \epsilon$	07.55	A_{0100}^{0100}	56.76	$\Phi_{0000}^{0300} \epsilon$
05.51	C_{1000}^{0000}	88.65	$A_{1100}^{0000} \epsilon$	04.80	$A_{0100}^{0100} \epsilon$	46.82	—
03.24	C_{0000}^{2000}	86.40	—	02.96	A_{0010}^{0100}	39.10	—
02.82	B_{0000}^{1000}	85.35	A_{0000}^{0001}	01.77	—	36.24	—
01.42	—	83.67	$(A_{0000}^{0001} \epsilon)$	00.59	—	22.54*	—
32 498.56	B_{0000}^{1000}	82.38	A_{1010}^{0000}	00.13	$A_{0010}^{0100} \epsilon$	22.08*	—
96.19	—	81.41	A_{2100}^{0000}	32 299.15*	—	20.16	A_{0000}^{0000}
95.05	—	79.73	$A_{1010}^{0000} \epsilon$	98.33	—	14.76	A_{1000}^{0000}
94.14	C_{0000}^{3000}	78.65	$A_{2100}^{0000} \epsilon$	97.48	A_{1100}^{0100}	10.18	A_{1000}^{0000}
92.41*	—	76.39	—	94.52	$A_{1100}^{0100} \epsilon$	04.41	A_{1000}^{1000}
91.22	—	75.62	A_{1001}^{0000}	93.13	A_{1100}^{0010}	00.16	A_{2000}^{0000}
88.25	B_{0000}^{2000}	73.53	$(A_{1000}^{0001} \epsilon)$	91.56	—	31 994.05*	A_{1000}^{2000}
84.84	—	72.43	A_{2010}^{0000}	90.29	$A_{1100}^{0010} \epsilon$	92.22	—
84.16	—	71.34	A_{3100}^{0000}	88.80	A_{0300}^{0000}	90.09	A_{3000}^{0000}
81.64	—	69.71	$A_{2010}^{0000} \epsilon$	87.71	A_{2100}^{0100}	80.11*	A_{4000}^{0000}
80.83*	—	68.71	$A_{3100}^{0000} \epsilon$	86.15	$A_{0300}^{0000} \epsilon$	66.65	—
77.95	B_{0000}^{3000}	65.61	A_{2001}^{0000}	84.75*	—	64.58	A_{0100}^{0000}
77.15	—	64.90	A_{0000}^{0000}	82.19*	A_{0300}^{1000}	58.79	A_{0100}^{1000}
74.42	—	64.23	—	79.50*	A_{0210}^{0000}	55.45	A_{0010}^{0000}
64.96	C_{0000}^{0100}	62.03	$A_{0000}^{0100} \epsilon$	78.89*	A_{1300}^{0000}	54.57	A_{1100}^{0000}
59.30	—	61.35	A_{4100}^{0000}	76.95	$A_{0210}^{0000} \epsilon$	49.63	A_{1100}^{1000}
57.94	A_{0000}^{0000}	59.12	A_{0000}^{0010}	76.07	$A_{1300}^{0000} \epsilon$	47.24	A_{0001}^{0000}
56.68*	A_{0000}^{0000} (wing)	56.21	$A_{0000}^{0010} \epsilon$	73.02*	$A_{0000}^{0200}, A_{0001}^{0000}$	45.50	A_{1010}^{0000}
55.22	$A_{0000}^{0000} \epsilon$	54.75	A_{1000}^{0100}	70.19	(A_{1210}^{0000})	44.51	A_{2100}^{0000}
52.26	A_{1000}^{0000}	53.55	$C_{0000}^{0300}, A_{1010}^{0000}$	68.81*	A_{2300}^{0000}	39.26	A_{2100}^{1000}
49.55	$A_{1000}^{0000} \epsilon$	52.58	—	66.81*	—	35.46	A_{2010}^{0000}
48.03	A_{1000}^{0000}	51.88	$A_{1000}^{0100} \epsilon$	66.16	$A_{2300}^{0000} \epsilon$		

Frequencies and assignments

frequency	assnmt.	frequency	assnmt.	frequency	assnmt.	frequency	assnmt.
31 934.54	A ₀₀₀₀ ³¹⁰⁰	31 514.19	a ₀₀₀₀ ⁰⁰⁰⁰	31 396.62	a ₁₀₀₀ ⁰²⁰⁰	31 132.41*	—
31.24*	—	12.47	a ₀₀₀₀ ⁰⁰⁰⁰ ε	93.92	a ₀₀₀₀ ⁰¹¹⁰	27.05	c ₀₀₀₀ ⁰¹⁰⁰
28.67*	A ₁₀₀₀ ³¹⁰⁰	10.62	a ₁₀₀₀ ⁰⁰⁰⁰ (wing)	92.73	a ₀₀₀₀ ¹²⁰⁰	20.41*	—
25.70*	A ₀₀₀₀ ³⁰¹⁰	08.83	a ₁₀₀₀ ⁰⁰⁰⁰ ε	86.30	a ₁₀₀₀ ¹²⁰⁰	18.92*	—
24.79*	A ₀₀₀₀ ⁴¹⁰⁰	06.95	a ₁₀₀₀ ⁰⁰⁰⁰ ε	83.78	a ₀₀₀₁ ⁰⁰⁰⁰ , (a ₀₀₀₀ ⁰¹⁰¹)	17.50*	c ₀₀₀₀ ¹¹⁰⁰
16.55*	—	03.97	a ₀₀₀₀ ¹⁰⁰⁰	82.42	a ₀₀₀₀ ²²⁰⁰ , a ₀₀₀₁ ⁰⁰⁰⁰ ε	12.63*	—
15.96*	A ₀₀₀₀ ⁴⁰¹⁰	02.18	a ₀₀₀₀ ¹⁰⁰⁰ ε	80.74	—	11.51	—
09.27	A ₀₀₀₀ ⁰²⁰⁰	31 498.30	a ₁₀₀₀ ¹⁰⁰⁰	79.41*	a ₁₀₀₁ ⁰⁰⁰⁰	09.68*	—
03.77	A ₁₀₀₀ ⁰²⁰⁰	96.35	a ₁₀₀₀ ¹⁰⁰⁰ ε	77.01*	a ₁₀₀₁ ⁰⁰⁰⁰ ε	03.00	—
02.33*	—	93.74	a ₀₀₀₀ ²⁰⁰⁰	75.33	—	01.65*	—
31 899.89	A ₀₀₀₀ ⁰¹¹⁰	91.88	a ₀₀₀₀ ²⁰⁰⁰ ε	73.54*	a ₀₀₀₁ ¹⁰⁰⁰	31 099.41	—
99.22	A ₀₀₀₀ ¹²⁰⁰	87.83	a ₁₀₀₀ ²⁰⁰⁰	72.26*	a ₀₀₀₀ ³²⁰⁰	98.17*	—
95.51	—	86.03	a ₁₀₀₀ ²⁰⁰⁰ ε	70.51	a ₀₀₀₀ ⁰¹⁰⁰	95.33*	—
93.58	A ₀₀₀₀ ⁰¹⁰¹	84.62*	—	68.72	a ₁₀₀₀ ⁰¹⁰⁰ ε	93.46*	a ₀₀₀₀ ⁰³⁰⁰
91.50	—	84.26	—	59.93	—	83.96	b ₀₀₀₀ ⁰⁰⁰⁰
90.80	A ₀₀₀₀ ⁰⁰²⁰	83.45	a ₀₀₀₀ ³⁰⁰⁰	58.94	a ₀₀₁₀ ⁰¹⁰⁰	80.76	b ₀₀₀₀ ⁰⁰⁰⁰ ε
89.90	A ₀₀₀₀ ¹¹¹⁰	81.77	a ₀₀₀₀ ³⁰⁰⁰ ε	58.36	(a ₀₀₁₀ ⁰¹⁰⁰ ε)	78.44	b ₀₀₀₀ ¹⁰⁰⁰
89.01	A ₀₀₀₀ ²²⁰⁰	75.78	(a ₁₀₀₀ ³⁰⁰⁰ ε)	55.71*	—	75.88	c ₀₀₀₀ ⁰⁰⁰⁰
86.41	A ₀₀₀₁ ⁰⁰⁰⁰	71.58	(a ₀₀₀₀ ⁴⁰⁰⁰ ε)	50.65	—	74.05	b ₁₀₀₀ ⁰⁰⁰⁰
84.86*	—	70.05*	—	48.86	—	72.79	c ₀₀₀₀ ⁰⁰⁰⁰ ε
84.25*	—	62.77	(a ₀₀₀₀ ⁵⁰⁰⁰)	47.79	a ₀₀₀₀ ⁰³⁰⁰	71.66	—
81.91	—	61.37	(a ₀₀₀₀ ⁵⁰⁰⁰ ε)	38.40	a ₀₀₀₀ ⁰²¹⁰	70.80	b ₁₀₀₀ ⁰⁰⁰⁰ ε
79.69*	A ₀₀₀₀ ²¹¹⁰	58.48	a ₀₀₀₀ ⁰¹⁰⁰	37.54	a ₀₀₀₀ ¹³⁰⁰	68.18	—
79.04*	A ₀₀₀₀ ³²⁰⁰	56.89	a ₀₀₀₀ ⁰¹⁰⁰ ε	27.13	a ₀₀₀₀ ²³⁰⁰	67.27	—
78.11*	—	52.67	a ₀₁₀₀ ⁰¹⁰⁰	23.18	—	64.14	c ₁₀₀₀ ⁰⁰⁰⁰
76.08	—	51.05	a ₀₁₀₀ ¹⁰⁰⁰ ε	31 292.79	a ₀₀₀₀ ⁰⁴⁰⁰	65.21	—
74.17*	A ₀₀₀₀ ⁰⁰⁰²	49.64	a ₀₀₁₀ ⁰⁰⁰⁰	70.65	—	64.15	b ₂₀₀₀ ⁰⁰⁰⁰
68.83	A ₀₀₀₀ ⁴²⁰⁰	48.23	a ₀₀₀₀ ¹¹⁰⁰	59.51	a ₀₀₀₀ ⁰⁰⁰⁰	63.09	c ₁₀₀₀ ⁰⁰⁰⁰ ε
67.64*	—	46.56	a ₀₀₀₀ ¹¹⁰⁰	54.50	a ₁₀₀₀ ⁰⁰⁰⁰	62.16	—
65.60*	—	43.76	a ₁₀₀₀ ¹¹⁰⁰	50.41	b ₀₀₀₀ ⁰⁰⁰⁰	60.93	b ₂₀₀₀ ⁰⁰⁰⁰ ε
65.08*	—	42.22	a ₁₀₀₀ ¹¹⁰⁰ ε	49.79	a ₁₀₀₀ ⁰⁰⁰⁰	56.27	c ₂₀₀₀ ⁰⁰⁰⁰
58.94*	—	40.58	a ₀₀₀₁ ⁰⁰⁰⁰	46.13*	b ₀₀₀₀ ¹⁰⁰⁰	50.96	(b ₀₀₀₀ ³⁰⁰⁰ ε)
56.61	—	39.43	a ₀₀₀₀ ¹⁰¹⁰	44.56	a ₁₀₀₀ ¹⁰⁰⁰	46.80	—
54.17	A ₀₀₀₀ ⁰³⁰⁰	37.96	a ₀₀₀₀ ²¹⁰⁰	40.93	b ₀₀₀₀ ¹⁰⁰⁰	40.95	(b ₀₀₀₀ ⁴⁰⁰⁰ ε)
44.54	A ₀₀₀₀ ⁰²¹⁰	35.72	a ₀₀₀₀ ²¹⁰⁰ ε	40.03	a ₀₀₀₀ ²⁰⁰⁰	29.08	b ₀₁₀₀ ⁰⁰⁰⁰
44.15*	A ₀₀₀₀ ¹³⁰⁰	34.96	—	31.33	b ₀₀₀₀ ²⁰⁰⁰	26.00	b ₀₀₀₀ ⁰⁰⁰⁰ ε
39.15*	—	33.24	a ₂₁₀₀ ¹⁰⁰⁰	21.77*	b ₀₀₀₀ ³⁰⁰⁰	23.51	b ₀₁₀₀ ¹⁰⁰⁰
37.05*	—	31.62	a ₂₁₀₀ ¹⁰⁰⁰ ε	03.94	a ₀₀₀₀ ⁰¹⁰⁰	19.33	b ₀₀₀₀ ¹¹⁰⁰ , b ₀₀₁₀ ⁰⁰⁰⁰
34.44*	A ₀₀₀₀ ¹²¹⁰	30.31	a ₀₀₀₀ ¹⁰⁰¹	31 197.82	a ₁₀₀₀ ⁰¹⁰⁰	16.48	b ₀₀₀₀ ⁰⁰¹⁰ ε
34.01*	A ₀₀₀₀ ²³⁰⁰	28.95	a ₀₀₀₀ ²⁰¹⁰	94.82	b ₀₀₀₀ ⁰¹⁰⁰	16.08	b ₁₁₀₀ ⁰⁰⁰⁰ ε
30.80*	A ₀₀₀₁ ⁰¹⁰⁰	27.69	a ₀₀₀₀ ³¹⁰⁰	94.08	a ₁₀₀₀ ⁰⁰⁰⁰	09.28	b ₂₁₀₀ ⁰⁰⁰⁰
23.84*	A ₀₀₀₀ ²²¹⁰ , (A ₀₀₀₀ ³³⁰⁰)	26.50	—	85.29	b ₁₀₀₀ ¹¹⁰⁰	08.48	—
16.15*	—	24.87	a ₀₀₀₀ ¹⁰⁰⁰ ε	82.56	c ₀₀₀₀ ⁰⁰⁰⁰	07.05*	—
31 799.35	A ₀₀₀₀ ⁰⁴⁰⁰	23.06	a ₂₀₁₀ ¹⁰⁰⁰	75.78	b ₂₁₀₀ ⁰⁰⁰⁰	06.13	b ₂₁₀₀ ⁰⁰⁰⁰ ε
89.26*	A ₀₀₀₀ ¹⁴⁰⁰	20.90	a ₀₀₀₀ ⁰¹⁰⁰	73.01	c ₁₀₀₀ ⁰⁰⁰⁰	03.16*	—
78.96*	A ₀₀₀₀ ²⁴⁰⁰	19.29*	a ₀₀₀₀ ⁰¹⁰⁰ ε	65.18	—	30 996.21	—
75.37*	A ₀₀₀₁ ⁰²⁰⁰	17.26	a ₀₀₀₀ ⁴¹⁰⁰	63.43	c ₀₀₀₀ ²⁰⁰⁰	93.08	—
59.90*	—	16.06*	—	62.36	a ₀₀₁₀ ⁰⁰⁰⁰	84.34*	b ₀₀₀₀ ⁰⁰¹⁰
55.43*	A ₀₀₀₁ ⁰⁰⁰⁰	14.00	a ₀₀₀₀ ⁰⁰¹⁰	53.88*	—	81.09*	b ₀₀₀₀ ⁰⁰¹⁰ ε
50.82*	—	12.42*	a ₀₀₀₀ ⁰⁰¹⁰ ε	51.01*	b ₀₀₁₀ ⁰⁰⁰⁰	74.68*	b ₀₂₀₀ ⁰⁰⁰⁰
44.48*	A ₀₀₀₀ ⁰⁵⁰⁰	03.92	a ₀₀₀₀ ¹⁰⁰⁰	48.66	a ₀₀₀₀ ⁰²⁰⁰	71.38*	b ₀₂₀₀ ⁰⁰⁰⁰ ε
42.56*	—	03.03	a ₀₀₀₀ ⁰²⁰⁰	39.50	b ₀₀₀₀ ⁰²⁰⁰	64.46*	b ₁₂₀₀ ⁰⁰⁰⁰
34.43*	A ₀₀₀₀ ¹⁵⁰⁰	31 399.49*	—	38.78	a ₀₀₀₀ ¹²⁰⁰	61.69	b ₁₂₀₀ ⁰⁰⁰⁰ ε

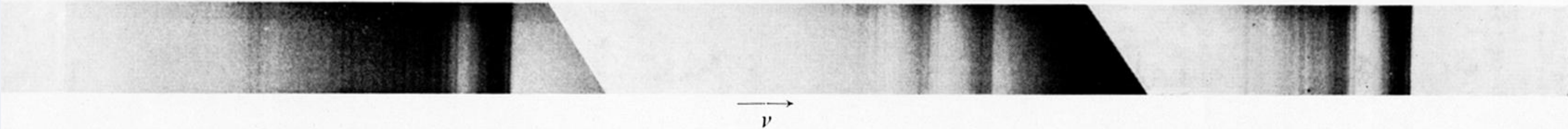


FIGURE 1. Composite enlargement of the spectrum of a part of the 3200 Å naphthalene system from photographs taken with the Hilger large quartz spectrograph. The bands are (right) the $1 \leftarrow 0$ band group $0 + 438 \text{ cm}^{-1}$, the ten times weaker $0 \leftarrow 0$ group (centre) at 32020 cm^{-1} , and the $0 \leftarrow 1$ band group $0 - 506 \text{ cm}^{-1}$ of about the same intensity as the $0 \leftarrow 0$. Individual bands are degraded to the red; and all the sequences strong enough to be seen are also degraded to the red, showing that the high-frequency band is always the principal band of the group, i.e. the first sequence member. The 10 and 55 cm^{-1} sequences are clearly visible in the spectrum.

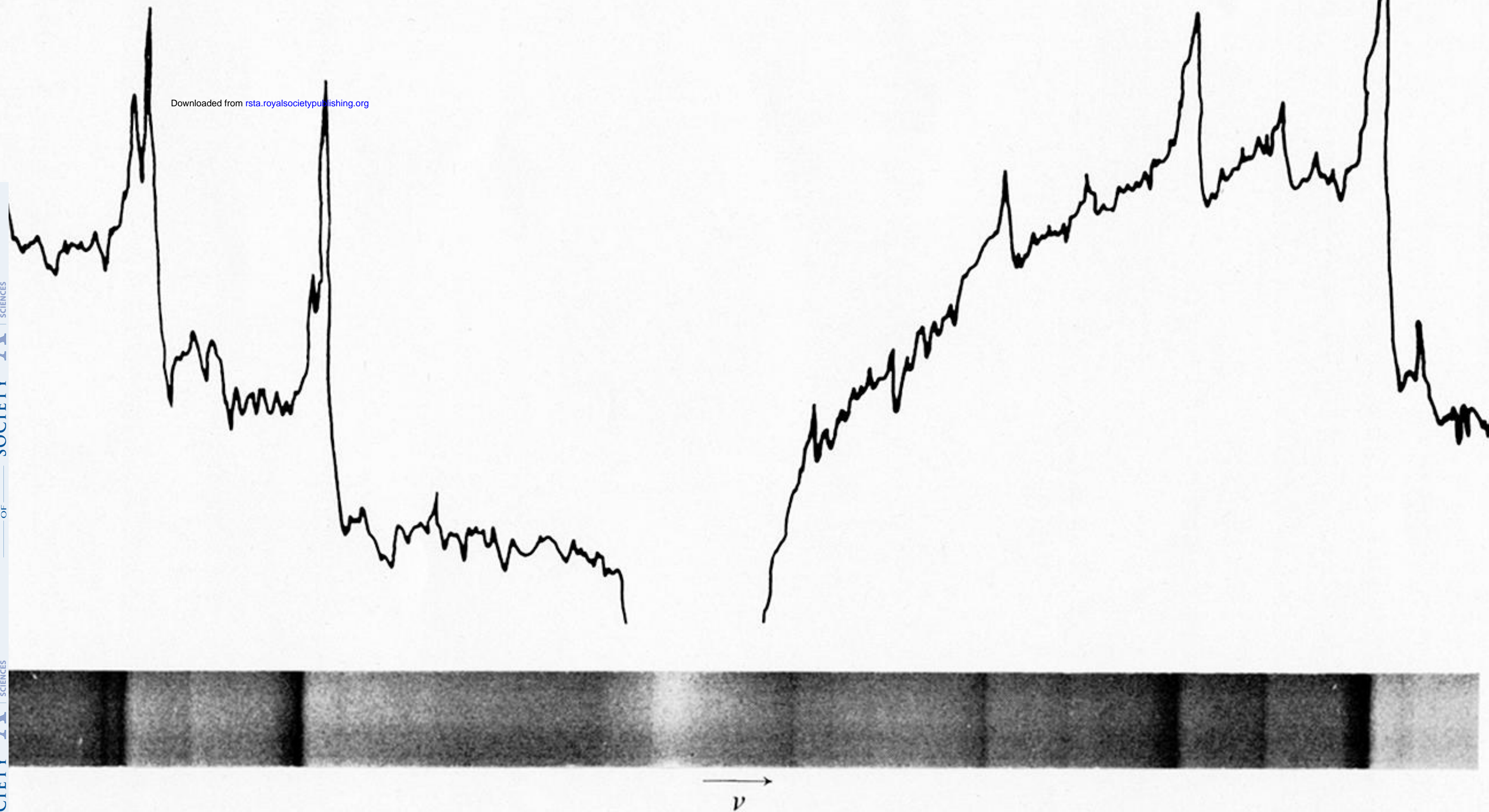


FIGURE 2. High-resolution photograph and microphotometer trace of part of the 0–0 band group near 32020 cm^{-1} . Several members of the 10 cm^{-1} sequence and one of the 55 cm^{-1} sequence are shown, each with the characteristic single head. The weaker bands lying between the main bands are $\nu'' - \nu'$ bands of about 5 cm^{-1} spacing. The band contours correspond to quasi-parallel *A*-type bands of an asymmetric rotor.

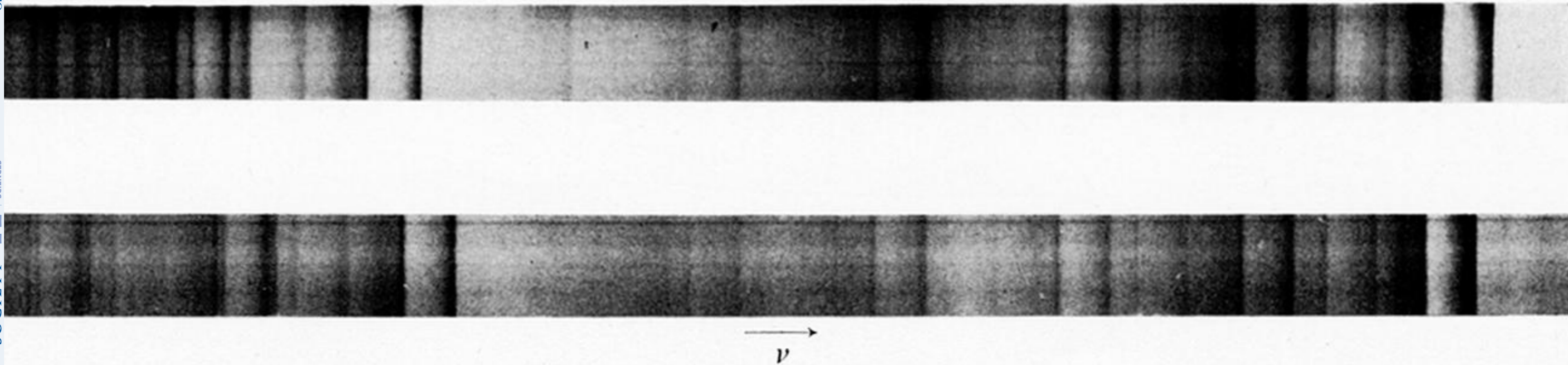


FIGURE 3. High-resolution spectra of parts of the $1 \leftarrow 0$ band group $0 + 438$ near 32458 cm^{-1} (top), and of the structurally similar $0 + 911$ near 32393 cm^{-1} (bottom). The characteristic double maxima of the bands are separated by $2.7\text{--}2.8 \text{ cm}^{-1}$. The contours are those of quasi-perpendicular B -type bands of an asymmetric-rotor.

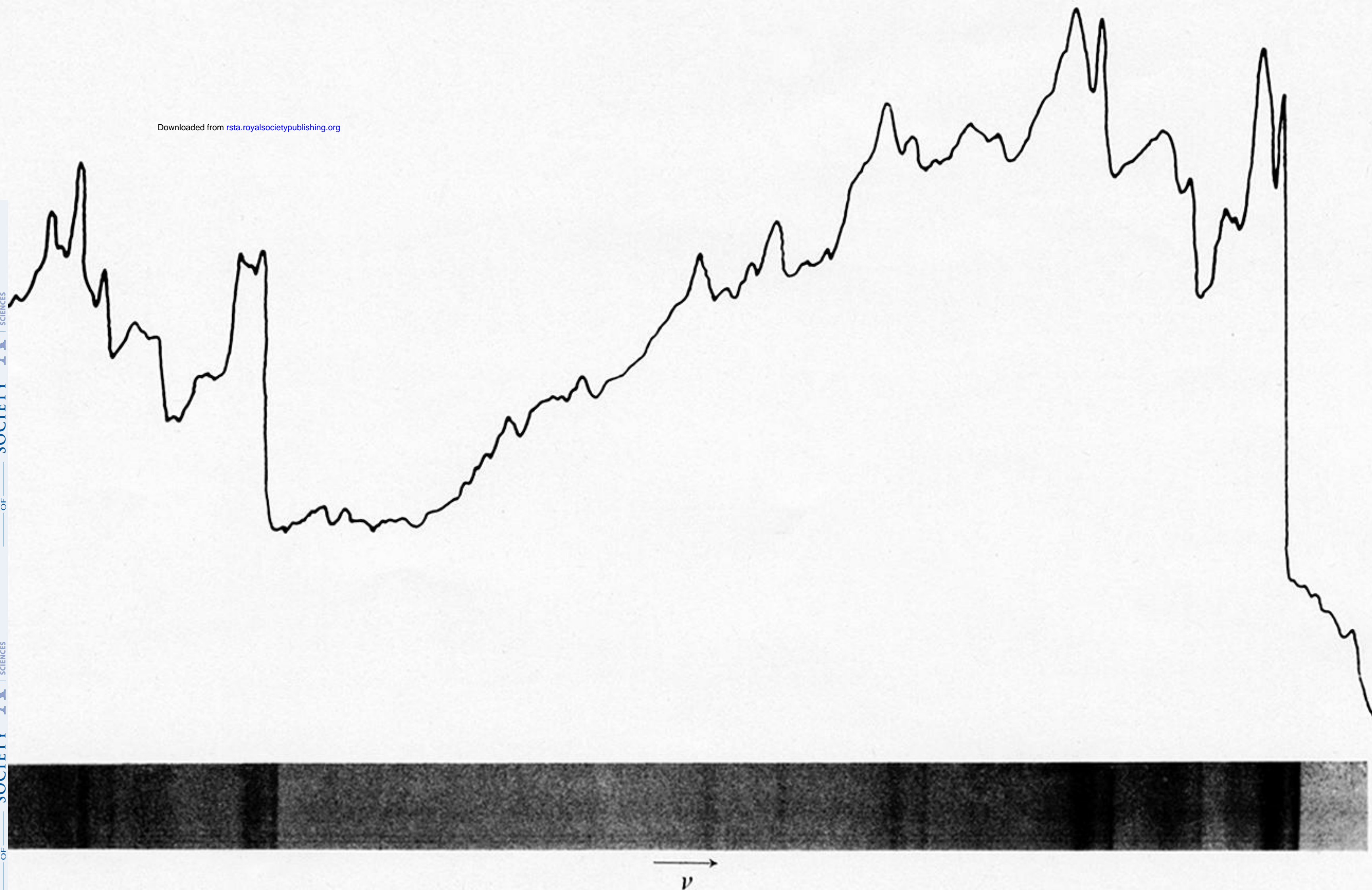


FIGURE 4. Part of the $0 \leftarrow 1$ band group $0 - 506 \text{ cm}^{-1}$ near 31514 cm^{-1} , showing the unique perturbed double-headed band contour found only in this band group.